



저작자표시-비영리-변경금지 2.0 대한민국

이용자는 아래의 조건을 따르는 경우에 한하여 자유롭게

- 이 저작물을 복제, 배포, 전송, 전시, 공연 및 방송할 수 있습니다.

다음과 같은 조건을 따라야 합니다:



저작자표시. 귀하는 원저작자를 표시하여야 합니다.



비영리. 귀하는 이 저작물을 영리 목적으로 이용할 수 없습니다.



변경금지. 귀하는 이 저작물을 개작, 변형 또는 가공할 수 없습니다.

- 귀하는, 이 저작물의 재이용이나 배포의 경우, 이 저작물에 적용된 이용허락조건을 명확하게 나타내어야 합니다.
- 저작권자로부터 별도의 허가를 받으면 이러한 조건들은 적용되지 않습니다.

저작권법에 따른 이용자의 권리는 위의 내용에 의하여 영향을 받지 않습니다.

이것은 [이용허락규약\(Legal Code\)](#)을 이해하기 쉽게 요약한 것입니다.

[Disclaimer](#)

Master of Science

WO₃ 히터가 있는 새로운 3 극 마이크로 퓨즈

A Novel Triode Micro Fuse with a WO₃ Heater

The Graduate School

of the University of Ulsan

School of Electrical, Electronic and Computer Engineering

Shovon Talukder

A Novel Triode Micro Fuse with a WO₃ Heater

Supervisor: Prof. Hyeon Cheol Kim

A Dissertation

Submitted to

the Graduate School of the University of Ulsan

in partial fulfillment of the requirements

For the degree of

Master of Science

by

Shovon Talukder

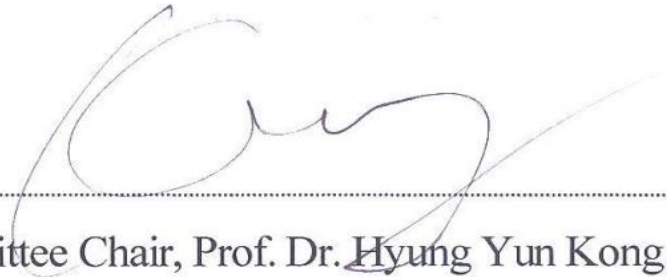
School of Electrical, Electronic and Computer Engineering

Ulsan, Republic of Korea

February 2022

A Novel Triode Micro Fuse with a WO₃ Heater

This certifies that the Master's Thesis
of Shovon Talukder is approved.



Committee Chair, Prof. Dr. Hyung Yun Kong



Committee Member, Prof. Dr. Hyeon Cheol Kim



Committee Member, Prof. Dr. Sung Jin Choi

Department of Electrical, Electronic and Computer Engineering

Ulsan, Republic of Korea

February 2022

Acknowledgement

All praise and thanks belong to almighty Paramatma.

I would like to express my sincere gratitude to my advisors Prof. Hyeon Cheol Kim of the School of Electrical Engineering at University of Ulsan for his supervisions, advice, continuous support, and consistent encouragement throughout my M.Sc. study and related research. His patience, motivation, immense knowledge, and continuous guidance helped me in all the time of research and writing of this thesis. Besides my advisors, I am gratefully indebted to my thesis committee: Prof. Dr. Hyeon-Cheol Kim, Prof. Dr. Chang-Woo Nam, Prof. Dr. Tae-Woo Kim, for their efforts to go through my thesis, insightful comments, and encouragement, which incited me to widen my research from various perspectives.

I am very much grateful to University of Ulsan for giving me such a wonderful research environment and financial support. This university gave me the chance to conduct several useful courses with excellent instructors that will give me a way to think and work properly in the rest of my life. I would like to express my hearties thanks to university and research center's staffs for their help and support. My special thanks go to Brain Korea 21Plus Program for its contribution and financial support during my study.

I would like to thank my fellow lab mates Mr. Md Mayen Uddin, Mr. Junhee Lee and Mr. Forhaz Farid in Smart Microsystem Laboratory for their friendship and support.

I am ever grateful to my mother Swapna Talukder and father Bidhan Chandra Talukder for raising me and helping me to achieve all that I have in my life. I would like to thank my younger brother Ankon Talukder for continuous support at the hard time. Last but not the least, I would like to thank my brothers, especially Morshed Mahmud, Md Jashim Uddin Shehab, Atish Bhattacharjee, Md Junayed Hasan, Niaz Morshedul Haque as well as extended family members, and close friends for their love, support and understanding.

University of Ulsan

February 2022

Shovon Talukder

Abstract

Portable electronic devices are comprised of a secondary battery or DC charge source and due to abrupt micro-current alteration and short circuit overcurrent; fire and explosions can happen. A protecting device should steadily cater to phenomena like overcurrent situation and micro-current alter state to avoid any hazardous circumstances. In this work, high current protecting multi-layered thin film triode micro fuses are designed and simulated using the MEMS-based tool of COMSOL Multiphysics software and then the device has been fabricated using the RF magnetron sputtering method and then electrically analyzed to compare between simulation and experimental data. To design a low melting point-based alloy for fuse element and negative temperature coefficient (NTC) based metal oxide functions as a heater material and to control high current high power is the primary purpose of this investigation. A Lead-tin (90Pb:10Sn) alloy has been employed as the low melting point-based fuse element and tungsten oxide (WO_3) is integrated with the layer as a self-heating resistor material. The electro-thermo-mechanical behavior is assessed, and a three-dimensional time-dependent modelling and simulation technique has been performed in both steady state and transient conditions with varying some physical and electrical parameters. The triode fuse simulated data shows that around 5.6A current the device temperature reaches to nearly 300°C and thus the triode fuse works by blowing the fuse. More importantly, after fabricating the device experimentally using nanofabrication technique, electrical characterization has been performed and experimental data almost provides similar result. The triode micro fuse device let current flow until 5A current, and the temperature distribution of the device follows simulated phenomena, thus blows at 5A current. This device completely suited for portable secondary battery protection system where current rating is like this device's rated current. This advanced research will facilitate a new class of portable micro fuse to be assembled with triode mechanisms in real-time technology for self-control protector.

Table of Contents

Acknowledgement	i
Abstract.....	ii
Table of Contents.....	iii
List of Figure.....	v
List of Tables	vi
CHAPTER 1 Introduction	
1.1 Motivation.....	2
1.2 Working principle.....	3
1.3 Thesis organization	3
CHAPTER 2 Design of triode micro fuse	
2.1 Literature Review	6
2.2 Design for triode micro fuse device materials	8
2.2.1 Conductive Electrode	8
2.2.2 Device Substrate	9
2.2.3 Heater Material.....	10
2.2.4 Fuse Element.....	12
CHAPTER 3 Modeling and simulation	
3.1 Theoretical study of NTC resistor’s transient state	14
3.2 Model and Analytical Assumption	19
3.2.1 Solid Mechanics	23
3.2.2 Electric Currents.....	23
3.2.3 Heat transfer in solids	24
3.2.4 Boundary condition.....	25
3.2 Simulation Result	26
CHAPTER 4 Fabrication of triode micro fuse	
4.1 Substrate Preparation.....	30
4.2 Silver Electrode Deposition	31
4.3 Heater Resistor deposition	32
4.4 Tin (Sn) deposition	33
4.5 Surface Resistance Measurement	34

4.6 The device fabrication process	35
CHAPTER 5 Electrical test and results	
5.1 Electrical characterization setup.....	37
5.2 Electrical characterization Analysis.....	38
CHAPTER 6 Conclusion and future work	
6.1 Conclusions	45
6.2 Future work and suggestions.....	46
6.3 List of Publications by the Author.....	46
References	47

List of Figure

Figure 2. 1 Portable device’s battery problem	7
Figure 2.2 Portable device’s hazardous situation	7
Figure 2.3. Motivation behind triode micro fuse device	7
Figure 2.4. Negative temperature coefficient of resistance behavior of Tungsten Oxide.	11
Figure 3.1. PSPICE ABM for NTCR with self-heating or joule heating effect for transient response investigation.....	17
Figure 3.2. Transient response of NTC resistant using analog behavioral model.....	18
Figure 3.3. Schematic of a cross sectional view of triode micro fuse	19
Figure 3.4. Material layers used in the modeling of triode fuse (Materials used to model the micro-fuse)	20
Figure 3.5. Design of triode micro-fuse structure (a) Silver electrode on Alumina Substrate (b) Tungsten oxide film on silver electrode (c) Pb-Sn alloy material on tungsten oxide and silver electrode (d) cross sectional view of the device with material appearance (e) top view of Material appearance of the device	22
Figure 3.6. Normal meshing of the triode micro-fuse (a) top view (b-d) cross sectional view	23
Figure 3.7. Temperature distribution of the triode micro fuse device maximum temperature and temperature profile	26
Figure 3.8. Temperature versus Current relationship of the micro fuse device by applying current through control and current electrode.....	27
Figure 3.9. Voltage distribution of the triode micro fuse device between control and current electrode.....	28
Figure 3.10. Isothermal contour distribution due to temperature on the micro fuse device.....	28
Figure 4.1. Optical image of Alumina Substrate	30
Figure 4.2. (a) Optical image of Silver (Ag) Target (b) Distance between the substrate and target in the RF magnetron sputtering chamber	31
Figure 4.3. Optical image of RF magnetron sputtering plasma during deposition process	32
Figure 4.4. Optical image of (a) Tungsten oxide (WO ₃) and (b) Tin (Sn) target for Sputtering.....	34

Figure 4.5. Four probe low resistance measurement system using KEITHLEY SCS-4200	34
Figure 4.6. Schematic diagram of the sputtered triode micro fuse device nanofabrication steps a) different masking design to deposit different film of silver, tungsten oxide and tin film b) Fabrication process of sputtered thin film c) photography of micro fuse under Cam Scope.....	35
Figure 5.1. Testing setup of triode micro fuse device for electrical characterization	37
Figure 5.2. Using thermocompression bonding at different temperature to attach the fuse material with the substrate/electrode/heater layer to form triode micro fuse device	38
Figure 5.3. Using silver conductive coating paste to form the bonding of fuse material with substrate/electrode/heater layer to form triode micro fuse device	40
Figure 5.4. Current-Voltage (I-V) characteristics of triode micro fuse device	41
Figure 5.5. Current-temperature characteristics of triode micro fuse	42
Figure 5.6. Triode micro fuse device blown at 5A applied current (a) before applied current (b) after applying the blown fuse.....	43

List of Tables

Table 2. 1 Electrical and Mechanical properties of different metal	9
Table 3. 1 Dimension of the material for geometry of micro-fuse	20
Table 3.2. Properties of Material	21
Table 4.1. Operating conditions of RF magnetron sputtering of Silver (Ag) target	32
Table 4.2. Operating conditions of RF magnetron sputtering of Tungsten oxide (WO ₃) target	32
Table 4.3. Operating conditions of RF magnetron sputtering of Tin (Sn) target	33

CHAPTER 1

INTRODUCTION

The Purpose of this chapter is to provide a general framework and introduction for the work presented in this master's thesis. This chapter is divided into three sections, addressing the research motivations, objectives, and thesis organization.

1.1 Motivation

Due to its high energy density and high current supply per unit mass and volume, high-capacity lithium-ion batteries (LIBs), which are employed not only in portable electronics, such as computers and cell phones but also attracting the most attention among electric or hybrid vehicles and energy storage systems. Actually, LIBs' superior performance and energy density have made them more attractive in all of these applications. Furthermore, LIBs now dominate the battery market for portable electronic devices due to their inherent benefits over other battery systems, including high specific capacity and voltage, reduced memory, outstanding cycling performance, low self-discharge, and a wide operating temperature range. However, the low safety performance of Electric Vehicles is now impeding the further expansion of the LIB market and its large-scale applications. Small and medium-sized secondary batteries used in portable devices have recently evolved into adequate forms to meet the demands of energy storage systems, such as reliable driving, long-term use, and rapid charging and discharging. However, frequent charging and discharging of lithium-ion batteries can result in unwanted overcurrent, overvoltage, overloads, and other issues. When a battery is overcharged or discharged or is subjected to an external or internal short circuit, it is vulnerable to electrical abuse, resulting in a sequence of unfavorable electrochemical processes. As a result, battery runaway, battery fire accidents and battery explosions are likely to be happened and lead a massive threat in the safety of users. In addition, substantial economic challenges for connected market sectors have arisen, as well as significant damage to LIBs' reputation taken placed. To avoid secondary battery fires and explosions caused by such electrical abuse, it is necessary to install a fuse that prevents current input by functioning when the incoming current rises from its rated value [1,2].

1.2 Working principle

Positive temperature coefficient (PTC) resistors and thermal fuses are the most common secondary protection devices. Although a PTC resistor can be controlled in both directions, problems such as delayed response time, finite breaking current, and significant leakage current must still be addressed [3].

In today's energy networks, a high-capacity electric fuse is essential [4]. Fuses have been used in low and medium voltage distribution network electrical installations for many years, and their behavior has been thoroughly investigated. They usually function at a lower current than their nominal current or under excess, or short-circuit, currents for a brief period. The Joule heating generated on the fuse element dissipates to the element's surrounding environment during operation [5].

We have developed a triode micro fuse by motivating from nanofabrication techniques and utilizing the advantage of excellent material available. The triode micro fuse device comprised of a stable substrate, conducting electrode, Negative temperature coefficient of resistance (NTCR) characteristics-based heater resistance, and an alloy as a fuse material.

In brief the objectives of this work are illustrated below:

- Self-heating or joule heating observation
- Heat transfer mechanism
- High current control mechanism in small size device
- Low melting point-based fuse material operation

This investigation and analysis are based on theory, simulation and experimental basis and the findings have been discussed thoroughly.

1.3 Thesis organization

The aim of this study is to show how the author's analysis was presented on theoretically, in a simulating manner and experimentally. The theoretical investigation, simulation based on parameter, fabrication techniques, electrical characterization of triode micro fuse device were all examined in depth. Furthermore, the capabilities of using this micro-fuse device on portable battery safety applications have been discussed. The thesis is organized as follows:

Chapter 1. Introduction

A short introduction and motivation behind the study, and overall works contents are illustrated in this section.

Chapter 2. Design of triode micro fuse

Backgrounds of this study along nanomaterials familiarization, design and the state of the art are discussed elaborately in this section.

Chapter 3. Modeling and simulation

The structure of the device along with the width, length, thickness of different layer material, electrical and mechanical properties, meshing of the device, physics that describes specific phenomena and their analysis were explained elaborately in this section.

Chapter 4. Fabrication of triode micro fuse

All experimental steps and device fabrications process along with the experimental tools and their processes were clarified extravagantly in this part.

Chapter 5. Electrical characterization setup and characterization analysis of triode micro fuse device

Chapter 6. Conclusion and future work

The overall outcomes of this research are summarized in this section. Additionally, some suggestions for the improvement of this model for high power and high current control applications were discussed and analyzed for the future work.

Design of triode micro fuse

Background and the necessity of this research, working mechanism, theoretical background to this research have been discussed in this chapter.

2.1 Literature Review

Li-ion Rechargeable (also known as secondary) batteries are becoming increasingly vital in the ongoing endeavor to minimize greenhouse gas emissions and promote the usage of renewable energy sources and energy transmitters. They make the energy derived from these sources more consistent and enable the use of this "green energy" in a much wider range of applications, such as in the automotive industry, where the number of electric (EV) and hybrid electric (HEV) vehicles is steadily increasing.

As a result, there is considerable interest in incorporating this efficient energy storage technology into other strategic systems, such as the main electrical grid, in the form of large stationary battery systems, and the aeronautical and aerospace industries, where high power and energy densities are required. Lithium ion (Li-ion) cells are a particularly intriguing alternative among the numerous types of rechargeable batteries available. They have already been steadily embraced in several applications such as mobile phones, portable computers, and many more. These batteries high energy density, high power density, and long cycle life, as well as other advantageous features like lack of memory effect and low self-discharge rate, making them ideal for a wide range of applications, particularly where high loads and small volumes are required.

However, in addition to a number of operational limitations, such as gradual capacity loss and the negative impact of temperature, a series of accidents, some of which occurred only recently, point to significant drawbacks and limitations in terms of reliability and, above all, safety, which hinders their adoption in a larger battery market. **Figure 2.1** illustrates the types of electrical abuse that occurs due to the frequent charging and discharging process of portable battery.

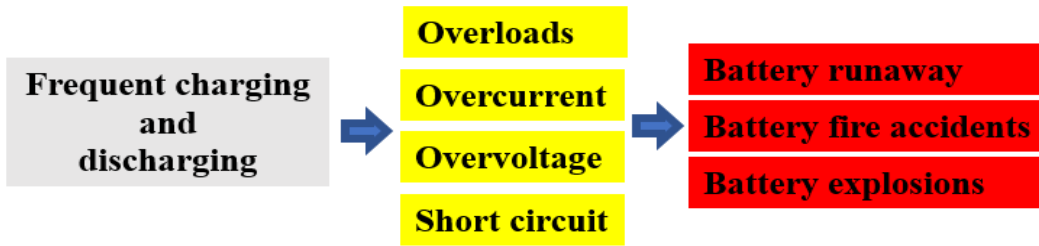


Figure 2. 1 Portable device’s battery problem

There have been numerous incidents of Li-ion batteries catching fire and exploding. Apart from electric vehicles fire incidents, other Li-ion battery-powered devices, such as notebook computers, hoverboards, and electronic cigarettes, have also been referenced in fire-related events. **Figure 2.2** shows incidents occurred due to the portable device battery problem.

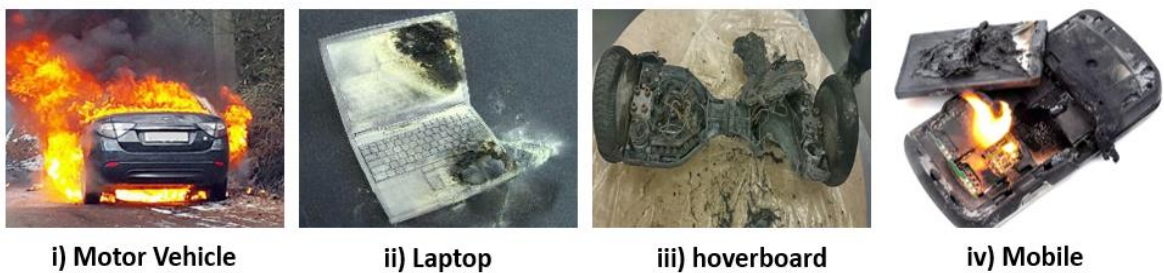


Figure 2.2 Portable device’s hazardous situation

The motivation can be demonstrated by the **Figure 2.3** where within small area high power-based device’s excess current can be interrupted by melting fuse element thus breaking the circuit rapidly.

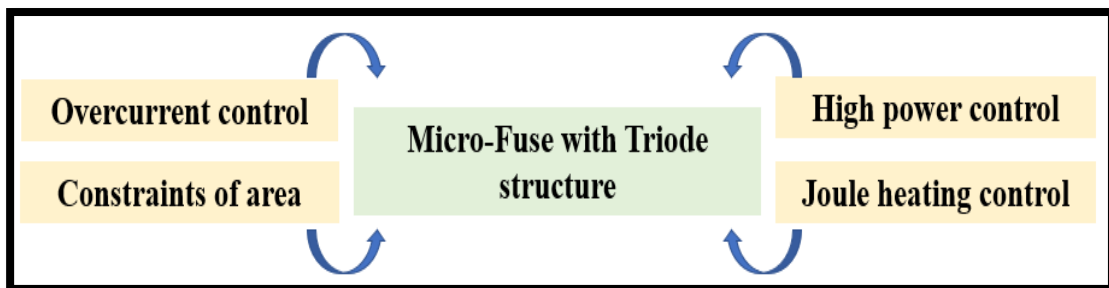


Figure 2.3. Motivation behind triode micro fuse device

Size limitation and lack of proper packaging of micro fuse device with the portable battery is one of the challenges that arises when it is crucial to design a protection system. And the micro

fuse device normally can control very low current which also hinders the applicability of the micro device in high power and high current applications. From using that motivation, a new triode structure based micro fuse device which can interrupt the high short circuit current, or overcurrent arises from overcharging and overvoltage.

2.2 Design for triode micro fuse device materials

2.2.1 Conductive Electrode

We have considered some parameters and attributes for selecting device material. Some of the attributes that conductive film materials should have include good electrical properties, thermal properties, solderability, high melting point, and low oxidation. Due to their low melting points, zinc, lead, and tin are not used as conductive materials. Copper has good thermal and electrical qualities, although it oxidizes easily at exalted temperatures. It might still be used provided the conductive film was shielded against oxidation, for as by utilizing inert protective coatings like graphene oxide-polymer composite [6]. Aluminum has poor thermal and electrical properties, and when exposed to air, it readily oxidizes. Gold has excellent thermal and electrical qualities, as well as chemical stability, but it has weak adhesive properties and is quite expensive. Silver has the best overall electro-thermal physical qualities of all the metals, including low electrical resistance, high thermal conductivity, a high melting point, and great oxidation resistance. Despite its relatively expensive cost, silver is widely believed to be the most widely utilized metal in semiconductor fuse design.

Mechanically, conductive film materials should have good adhesion to the substrate, a low Young's modulus, a thermal expansion coefficient that is preferably comparable to that of the substrate, a high yield stress, and a high creep strength. The thermal expansion coefficients of silver, gold, and copper are all insignificant. Silver and gold have the least yield stress of the three metals. Zinc and lead both have strong thermal expansion coefficients and lead also has a low yield stress. Because metals with high electrical conductivity typically have low adhesion to substrates, neither silver nor copper have particularly good adhesion to ceramic substrates. To improve the adhesion property, intermediate layers of Vanadium, chromium, or nickel might be utilized [7]. Copper and probably silver are the only metals with mechanical characteristics that are attractive.

2.2.2 Device Substrate

The substrate acts as a mechanical platform for the element, as well as a heat conductor for the current-carrying conductive layer. As a result, superior thermal properties at ambient and working temperatures are preferred, but less favorable thermal properties at high temperatures are undesirable. This is because an increase in the thermal time constant speeds up the fuse action at high temperatures, which occur under short circuit situations. Excellent Electrical insulation properties, high melting point, good mechanical strength, good resistance to thermal shock, relative high surface smoothness have been considered to choose the substrate material. High surface smoothness is very essential if the thickness of the conductive film is small. Polished alumina exhibits small grain size and thus provides better surface smoothness. However, in other applications, such as electroless plating, a somewhat high surface roughness might be desirable since it allows for effective mechanical bonding. But depending on the pre arching thermal absorption capability, alumina suits more as a substrate material.

Hence, Silver films on alumina substrates were chosen as the conductive film and substrate material for this study because they were thought to have the best overall electro-thermo-mechanical properties.

The details of the electro thermal properties and mechanical properties have been listed on **Table 2.1** below.

Table 2. 1 Electrical and Mechanical properties of different metal

Material	Electro Thermal Property			Mechanical Property		
	Electrical Resistivity	Thermal Conductivity	Melting Point	Thermal Expansion Coefficient	Young's Modulus	Yield stress
	10^{-8} Ohms/m	W/m [°] C	°C	10^{-6} °C ⁻¹	GN/m ²	MN/m ²
Silver	1.47	428	961	19.1	82.7	29.4
Copper	1.55	403	1083	17	130	69-287
Gold	2.05	319	1063	14.1	78.5	29.4-39.2
Aluminum	2.5	236	659	23.5	70.6	35.3
Zinc	5.5	117	420	31	104.5	104
Tin	11.5	68	232	23.5	49.9	N/A
Lead	19.2	36	328	29	16.1	4.9-9.8

2.2.3 Heater Material

Thermally sensitive semiconductor resistors with a considerable reduction in resistance as temperature rises are known as negative temperature coefficient of resistance (NTCR). When a current pass through the NTC resistance, however, it heats up due to power dissipation [8]. Resistance follows an exponential law in terms of temperature dependency. These resistor's NTC feature makes them ideal for use as thermistors in temperature sensing and continuous overheat detection applications [9].

The resistance variation with temperature is measured using the temperature coefficient of resistance (TCR), dR/dT . Positive temperature coefficient of resistance (PTCR, $dR/dT > 0$) represents the increase in resistance as temperature rises, while negative temperature coefficient of resistance (NTCR, $dR/dT < 0$) indicates the decrease in resistance as temperature goes up [10]. NTC resistors are made up of multivalent transition metal oxides like WO_3 , NiO, Mn_3O_4 , Co_3O_4 , Cu_2O_3 , and Fe_2O_3 , which produce a complex spinel (W, Mn, Co, Fe, Cu) $_3O_4$ structure for more dependable sensor applications[11]. NTC resistors perform because when the temperature rises, the number of active charge carriers released from the crystal lattice increases. The material for the NTC resistor is determined by several criteria, one of which is the temperature range demanded. Temperatures in the range of 1 to 100°K are commonly employed with germanium NTC resistors. NTC resistor made of silicon can withstand temperatures of up to 250°K. For the temperature range of 200 to 700°K, metallic-oxide NTC resistors are employed. Very stable compounds are still necessary at higher temperatures, and NTC resistors for these temperatures can be manufactured from materials such as WO_3 , Al_2O_3 , BeO, MgO, ZrO_2 , Y_2O_3 , and Dy_2O_3 .

WO_3 is a transition metal oxide, and its lattice can withstand a considerable amount of oxygen deficiency where only a partial loss of the WO_3 oxygen content is needed to affect its electronic band structure and increase its conductivity by a large amount. Depending on the stoichiometry, the electrical conductivity of single-crystal WO_3 ranges from 10 to 10^{-4} Scm^{-1} . As a result, the electrical characteristics of WO_3 are highly influenced by synthesis techniques and growth environments[12].

Chemical and physical deposition technologies such as electrospinning[13], spray pyrolysis[14], electrodeposition[15], thermal evaporation[16], plasma aided evaporation[17], and DC and RF magnetron sputtering techniques[18] have all been utilized to fabricate WO_3

films. Magnetron sputtering, for example, has the advantage of depositing uniform coatings on wide areas of substrates, a high degree of film adhesion, and relatively simple scalability properties. By using RF magnetron sputtering the tungsten oxide films have been fabricated in low temperature condition.

To understand and evaluate the NTC characteristics of WO_3 metal oxide film three samples of different thickness has been examined under temperature ranges from room temperature to 600K. The relation between resistance and temperature has been plotted and shown in **Figure 2.4**.

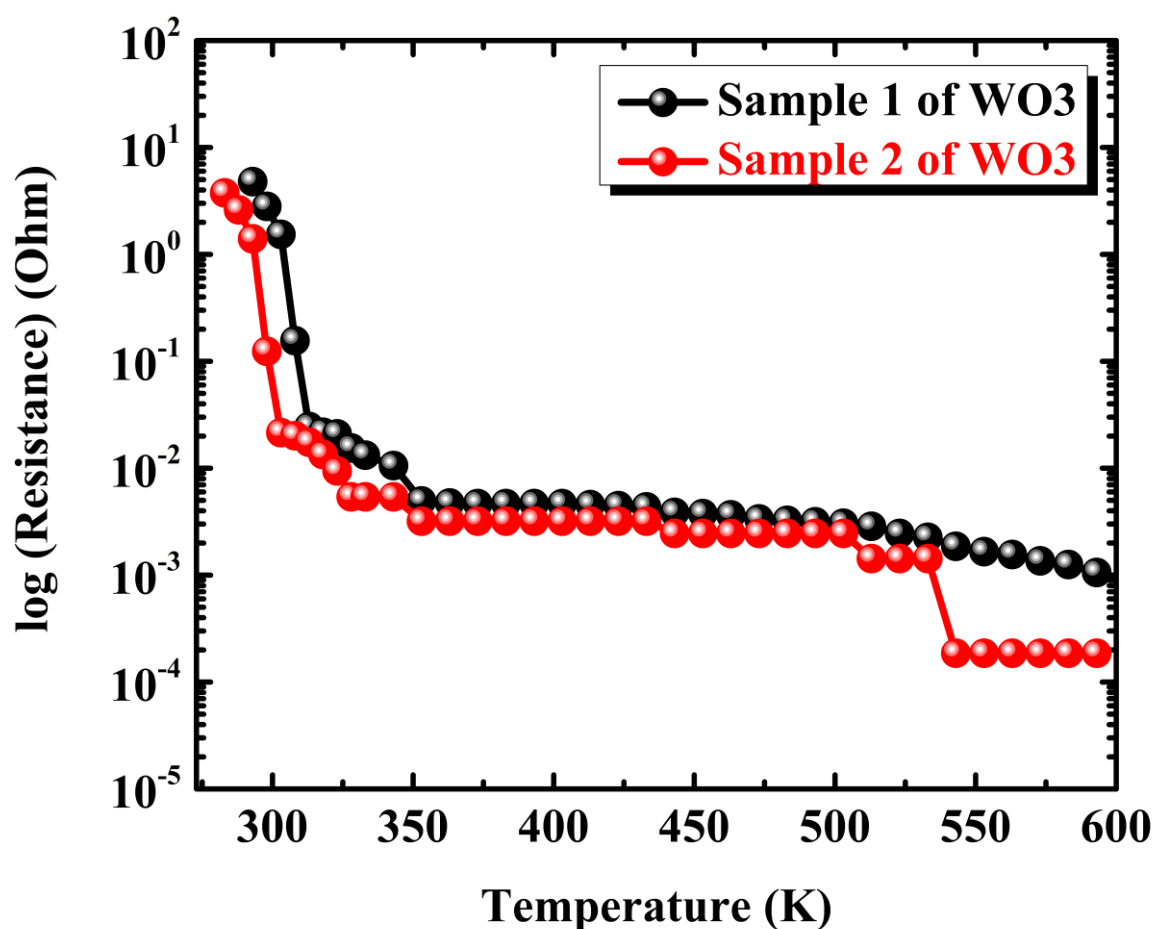


Figure 2.4. Negative temperature coefficient of resistance behavior of Tungsten Oxide.

In this figure, we can observe that all samples have shown similar characteristics of rapid decreasing of resistance with the increasing temperature till 320K and then it decreases very slowly with the increasing temperature. From this figure, negative temperature coefficient of resistance of tungsten oxide metal oxide can be calculated.

2.2.4 Fuse Element

To create the protective fuse circuit, a metal must be manufactured in such a way that it melts when exposed to the heat of the heater resistance. A high resistance and low melting point-based alloy could meet that requirement of the fuse material. Tin based alloy like 90Pb-10Sn has the melting point 275-302°C (548-575K). Conditions for bonding low melting point metals to be used as fuse solubilizers require properties such as ensuring sufficient insulation distance after fuse alloy are melted by over-current and over-voltage and satisfying fuse properties.

Normally when current passes through a conducting path then heat is generated and due to the heat dissipation, the designed fuse material melts. For a small amount of current flow this fuse can be melt and this interrupts the application of thin film micro fuse for high current and high-power applications. However, if any transitional negative temperature coefficient of resistance-based metal oxide is used between the conductor of the current and the fuse material which can perform triode mechanism then the application of thin film micro fuse can be enhanced. If self-heater resistance gets heated due to the electric current passing through the conducting path, then it preserves a uniform temperature distribution during heating, then its total resistance would reflect its accurate temperature. In normal rated current the fuse will not be interrupted because of having self-heater heater resistance in the system. When overcurrent or abnormal current passes through the conducting path then self-heater resistance shows it's NTC characteristics thus decreasing resistance with the increasing temperature, meanwhile raises the resistor's temperature over that of its surroundings, increasing the conductivity through NTC material and finally melting the fuse element, preventing the over current from traveling through the conducting route.

A micro fuse fabricated by integrating Al/CuO-based nano energetic materials on a micro wire tested by open-air combustion technique and also characterized [19]. A micro copper fuse on glass epoxy plate developed using wet etching technology where numerical simulation was studied and fuse characteristics were evaluated experimentally [20]. A thin-film micro-fuse with a novel structure based on Ag deposition on the diarylethene (DAE) surface proposed and characterized [21]. Here, indigenously formulated lead free thick film NTC thermistor for the self-heating applications was reported [22]. To get the complete static current-voltage characteristic of a thermistor including the self-heating effect, an analog behavior model was presented as loaded and unloaded thermistors with NTC phenomena [8].

Modeling and simulation

To develop the triode micro fuse device and to understand the physical mechanism of the device a simulation model and geometry will be presented on this chapter. Prior to that the theoretical background of taking the consideration of choosing NTC of resistance-based metal oxide as a heater material will be discussed.

3.1 Theoretical study of NTC resistor's transient state

Thermally sensitive semiconductor resistors with a considerable reduction in resistance as temperature rises are known as negative temperature coefficient of resistance (NTCR). In some circumstances, The NTC element is considered as a fixed resistor, with R_T varying with ambient temperature T_A .

$$R_T = R_N \exp\left(\frac{\beta}{T_A} - \frac{\beta}{T_N}\right) \quad (1)$$

Where, β = Material Constant, R_N = Resistance at the Nominal temperature T_N (in Kelvin).

When a current passes through the NTC resistor, however, it heats up due to power dissipation.

When an NTC resistor is placed in an electrical circuit, power is dissipated as heat, and the resistor's body temperature rises above its surrounding's ambient temperature. Energy must be supplied at a rate that determines the rate at which it is lost plus the rate at which it is absorbed (the energy storage capacity of the device).

$$\frac{dH}{dt} = \frac{dH_L}{dt} + \frac{dH_A}{dt} \quad (2)$$

In an electrical circuit, the rate at which thermal energy is provided to the NTC resistor is equal to the power dissipated in the NTC resistor.

$$\frac{dH}{dt} = P = I^2 R = EI \quad (3)$$

The rate of thermal energy loss from the NTC resistor to the environment is proportional to the resistor's temperature rise.

$$\frac{dH_L}{dt} = \delta \Delta T = \delta(T - T_A) \quad (4)$$

Here, (T) is the instantaneous temperature and (T_A) is the ambient temperature. The dissipation constant (δ) is defined as the ratio of a change in the power dissipation of a NTC resistor to the resulting body temperature change at a given ambient temperature. The dissipation constant is determined by the thermal conductivity, the relative motion of the medium in which the NTC resistor is placed and heat transmission from the resistor to its surroundings via conduction through the leads, free convection in the medium, and radiation. Because it varies significantly with temperature and temperature rise, the dissipation constant is not a real constant. It's usually measured in a state of equilibrium. The rate at which the NTC resistor absorbs thermal energy to cause a certain quantity of temperature rise can be represented as follows:

$$\frac{dH_A}{dt} = sm \frac{dT}{dt} = C_{th} \frac{dT}{dt} \quad (5)$$

Where, (s) is the specific heat, and (m) is the NTC resistor's mass. The heat capacity (C_{th}) of a resistor is the product of its specific heat and mass, and it is determined by the materials and structure of the NTC resistor. As a result, the heat transfer equation for an NTC resistor at any point in time after power is provided to the circuit is followed equation:

$$P = \frac{dH}{dt} = \delta(T - T_A) + C_{th} \frac{dT}{dt} = VI \quad (6)$$

Here, $\frac{dH}{dt}$ is the change of stored thermal energy with respect to time.

We must analyze NTC resistor behavior under transient and steady state situations to accomplish the analysis of thermal characteristics of NTC resistors. When the power (P) is constant, the solution to equation (6) is:

$$\Delta T = (T - T_A) = \frac{P}{\delta} [1 - \exp \left\{ \frac{-\delta}{C} t \right\}] \quad (7)$$

Equation (7) demonstrates that a NTC resistor's body temperature will rise above the ambient temperature as a function of time when a substantial amount of power is dissipated in it.

By using this equation, we have designed the PSPICE Analog behavioral model to understand the transient behavior of NTC resistor. **Figure 3.1** represents NTC resistor Analog behavioral model (ABM) with the transient state characteristics using PSPICE simulation package. In the figure, based on the detected current multiplied by the NTC resistance, E1 generates the voltage across the "NTC resistor" where V2 denotes ambient temperature 20°C. E3 symbolizes the changes of temperature or the temperature variation as a function of time which is the transient response or transient state of the system. Voltage source V1 worked to recognize the current while V3 is necessary with R1, R2 resistance to get the desired output.

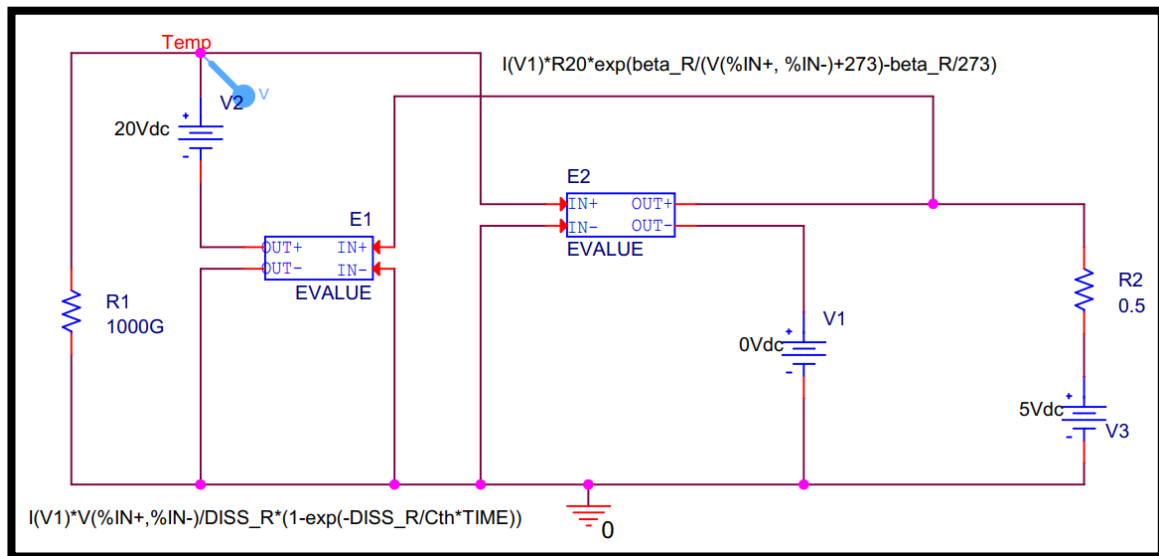


Figure 3.1. PSPICE ABM for NTCR with self-heating or joule heating effect for transient response investigation

When $dT/dt=0$ in equation (6) or $t \gg C/\delta$ in equation (7), a state of equilibrium is achieved. The rate of heat loss is equal to the power provided to the NTC resistor in this steady state situation. Therefore:

$$\delta(T - T_A) = \delta\Delta T = P = E_T I_T \quad (8)$$

Here, (E_T) is the steady state or static NTC resistor voltage and (I_T) is the steady state current. The Voltage-Current Characteristic is governed by this equation.

The heat transfer equation can be rewritten as follows when the power in a NTC resistor is reduced to a level where self-heating is regarded negligible,

$$\frac{dT}{dt} = \frac{-\delta}{C} (T - T_A) \quad (9)$$

This is simply Newton's Law of Cooling, and its solution is,

$$T = T_A + (T_I - T_A) \exp\left\{\frac{-t}{\tau}\right\} \quad (10)$$

In equation (10), (T_I) is the initial body temperature, (T_A) is the ambient temperature and (τ) is the thermal time constant of the device and $\tau=C/\delta$ [23]. The thermal time constant is influenced by the same environmental elements as the dissipation constant, notably NTC resistor's size, shape, and leads, as well the medium's thermal conductivity and velocity, conduction via the leads, free convection in the medium, and radiation losses. To get the output of the circuit constructed in **Figure 3.2**, different dissipation factor has been considered to understand the transient state of the model. **Figure 3.2** shows the output of ABM circuit showing the transient

state of NTC resistor temperature as a function of time. In this figure NTC resistance influenced by different dissipation factor of 0.5mF to 1.5mF which validates the equation 7.

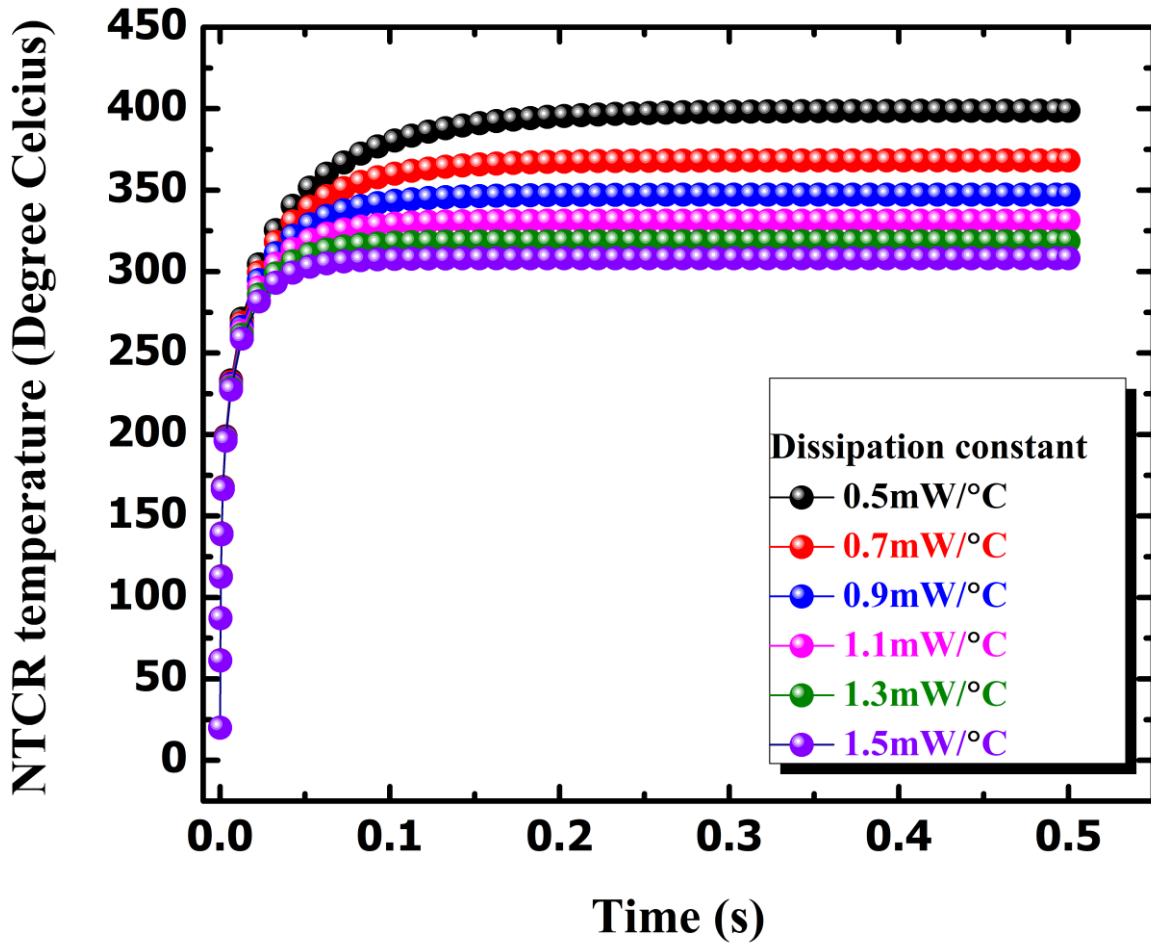


Figure 3.2. Transient response of NTC resistant using analog behavioral model.

3.2 Model and Analytical Assumption

After getting the transient response of NTCR it is required to perform finite element modelling of four layers for analytical assumption.

The main theme of this work is to analysis of effects of incoming current of the micro-fuse, relationship between temperature vs current, voltage and how much current is needed to melt the fuse material to fully protect the circuit from overcurrent. Here, for the first time, Tungsten oxide/Pb-Sn alloy based micro fuse structure on silver electrode has been designed. Tungsten oxide film works as a NTC heater resistor and Pb-Sn alloy as a low melting point-based fuse material. Conducting and aspects such as electric potential, temperature profile are studied by using COMSOL Multiphysics. Here, we conclude that this micro-fuse structure concept that combines fuse mechanism with triode structure can be applied in many electrical, electronic, and industrial applications.

This work mainly approached on the modeling and optimization of different heater thickness and different fuse alloy thickness and thus to find the amount of current needs to reach the melting temperature of the fuse material. **Figure 3.3** shows the cross-sectional view of the triode micro fuse. **Figure 3.4** depicts a cross-sectional view with each layer identified by a different color mentioning with the melting point, boiling point, and density.

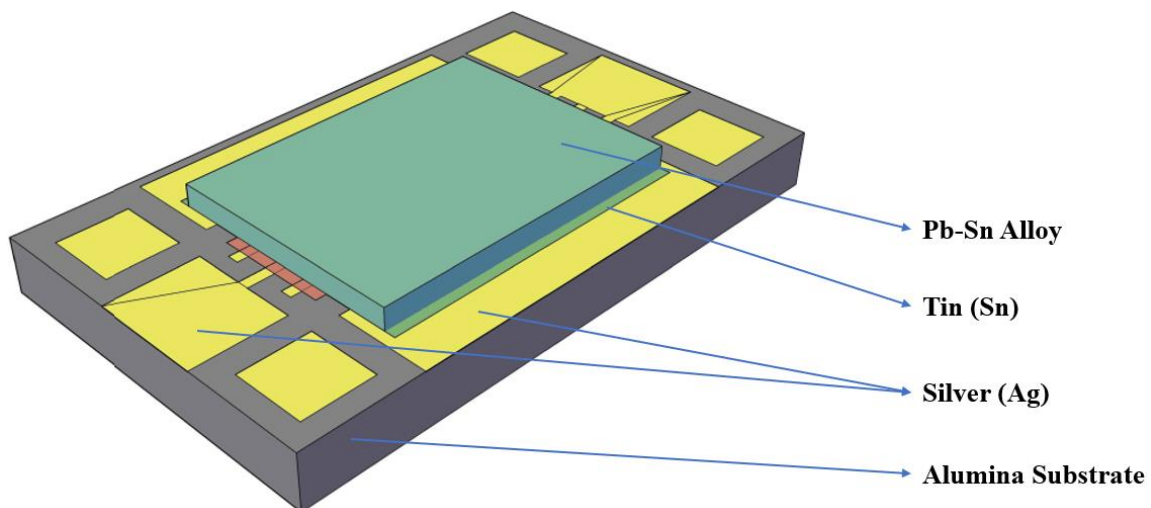


Figure 3.3. Schematic of a cross sectional view of triode micro fuse

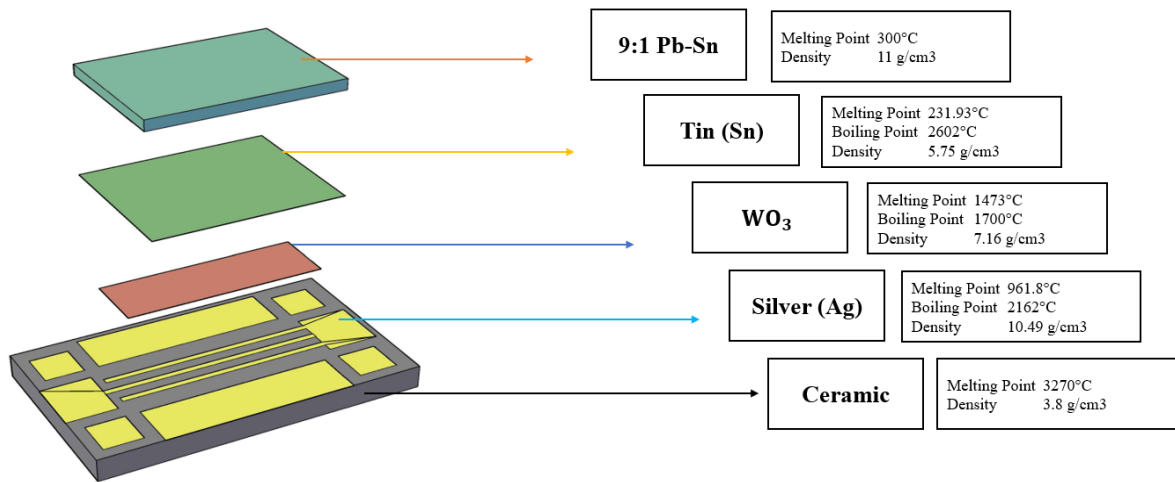


Figure 3.4. Material layers used in the modeling of triode fuse (Materials used to model the micro-fuse)

To design the micro-fuse different material's geometry are mentioned in **Table 3.1**. The fuse material is select based on the withstand capacity of low temperature melting mechanism. The total fuse geometry is $5.4 \times 3.2 \text{ mm}^2$ in length \times width and 0.7 mm in thickness and that is shown in **Table 3.1**.

Table 3. 1 Dimension of the material for geometry of micro-fuse

Parameter	Alumina Substrate (Al ₂ O ₃)	Silver (Ag) electrode	Tungsten Oxide (WO ₃) heater	Tin (Sn)	Lead-Tin (Pb-Sn) fuse
Length (mm)	5.4	-	3	3	3
Width (mm)	3.2	-	1	2.4	2.4
Thickness (mm)	0.7	0.001	0.002	0.001	0.1

The properties of materials used in this analytical simulation are tabulated in **Table 3.2**. In this section the design and simulation are performed based on these parameters. The structural design has been shown in **Figure 3.5**. In **Figure 3.5 (a-c)** the conductive electrode, heater and fuse material physical design have been shown. **Figure 3.5 (d-e)** is the device appearance after declaring the material properties of **Table 3.2**.

Table 3.2. Properties of Material

Parameters	Al ₂ O ₃	Ag	WO ₃	Sn	Pb-Sn
Young's modulus (Pa)	3×10 ¹¹	8.30×10 ¹⁰	7.40×10 ¹⁰	4.16×10 ¹⁰	2×10 ¹⁰
Poisson Ratio	0.22	0.365	0.49	0.33	0.43
Density (Kg/m ³)	3800	10497	7160	7250	10750
Thermal conductivity (W/m-k)	20.3	429	1.63	53.5	25
Heat capacity at constant pressure (J/Kg-k)	880	239	315.34	230	140
Electrical conductivity (S/m)	1×10 ⁻¹²	62.1	434.78	5.8823	5.15×10 ¹⁶

The analytical module on solid mechanics, electric currents, and heat transfer in solids is used to build the micro-fuse structure to achieve the desired findings that are available when using the Finite Element Method approach. Normal meshes are configurable because active layers influence the shape and size of the mesh. **Figure 3.6** depicts top view of 3D normal meshing of the device with cross sectional view.

In this simulation, (1-5.6) A current is applied on the electrode of the micro fuse. The effects of applied current on potential, temperature, resistance is quantitatively investigated.

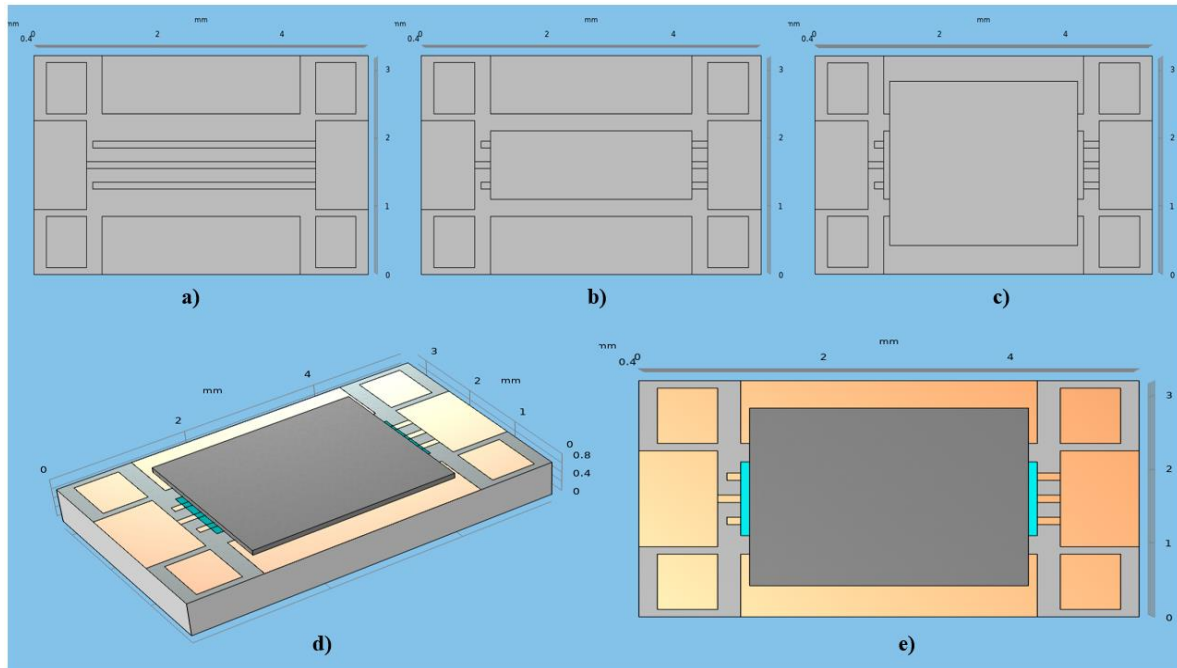


Figure 3.5. Design of triode micro-fuse structure (a) Silver electrode on Alumina Substrate (b) Tungsten oxide film on silver electrode (c) Pb-Sn alloy material on tungsten oxide and silver electrode (d) cross sectional view of the device with material appearance (e) top view of Material appearance of the device

For the simulation of micro-fuse, the Joule Heating and Thermal Expansion interface is studied where three major physics incorporates Multiphysics effects such as solid mechanics, electric currents, and heat transfer in solids. The electromagnetic losses from the electric field as a heat source are added by the predetermined interaction.

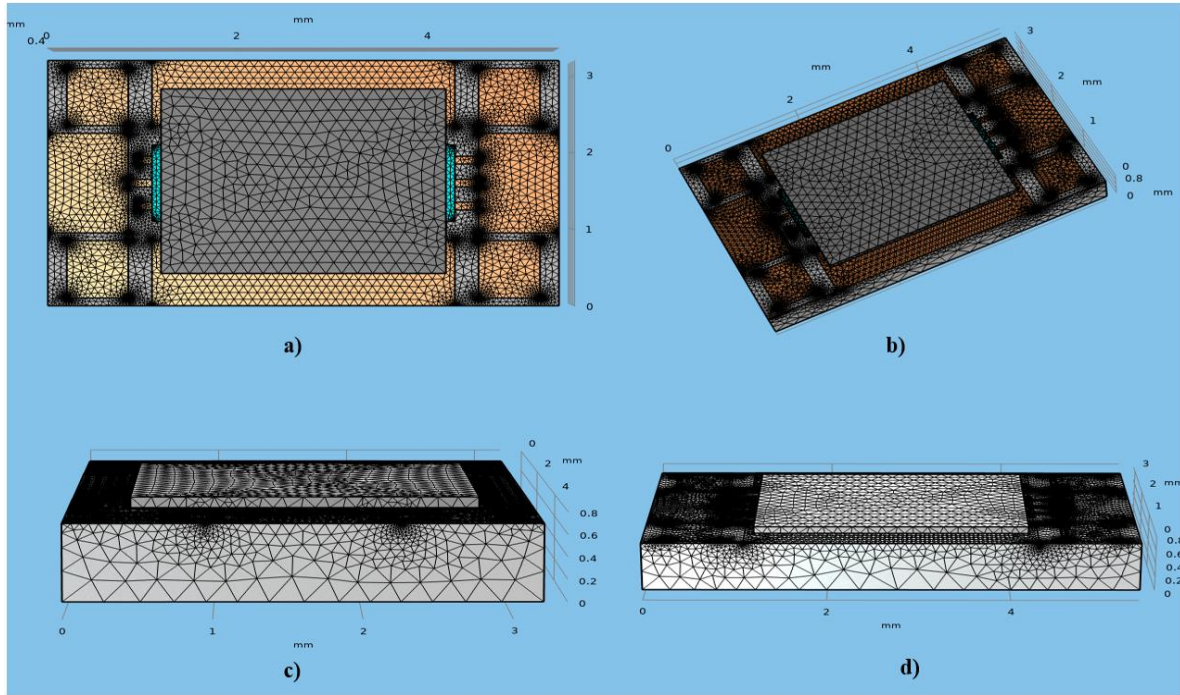


Figure 3.6. Normal meshing of the triode micro-fuse (a) top view (b-d) cross sectional view

3.2.1 Solid Mechanics

The temperature of the Heat Transfer in Solids interface also acts as a thermal load on the Solid Mechanics interface, inducing thermal expansion. The Solid Mechanics interface is built on solving equations of motion in tandem with a solid material constitutive model. Displacements, stresses, and strains are computed as a resultant. Following the successful creation of the fuse device, it is necessary to combine it into a single device using the union function from a Boolean expression.

3.2.2 Electric Currents

To compute the electric field, current and potential distribution in conducting electrode constant voltage and constant current both modes have been employed. Both approaches yielded the same result: the resistance of WO₃ reduced when the heating power was raised and this can be explained based on Poisson's equation,

$$-\nabla^2 V = 0 \quad (11)$$

The physics interface uses the scalar electric potential as the dependent variable to solve a current conservation equation based on Ohm's law.

3.2.3 Heat transfer in solids

The proposed device's operating temperature transmits heat via heat conduction between the conductive electrode and the heater material layer, then raises the temperature by lowering the resistance, indicating NTC properties, and finally absorbs the heat as a self-heating mechanism. It melts the fuse material and instantaneously stops the current at the optimum temperature. The minus diagonal in temperature is precisely proportional to the temperature of the material we specified, according to Fourier's rule, which is a principle that determines heat conduction is

$$\vec{q}^n = -k\vec{\nabla}T \quad (12)$$

Where, k is the solid thermal conductivity, q^n is flux density and T is the device temperature. Then the equation can be written as

$$q^n = -k \left[i \frac{dT}{dx} + j \frac{dT}{dy} + k \frac{dT}{dz} \right] \quad (13)$$

In the n direction we can write

$$q_n^n = -k\vec{\nabla}T \quad (14)$$

So, the heat flux in all direction can be written as

$$q^n = iq_x^n + iq_y^n + iq_z^n \quad (15)$$

3.2.4 Boundary condition

To successfully evaluate the simulation of the fuse device, the base of the micro fuse and one corner of the fuse has been fixed under the module of fixed constraint of solid mechanics. For electrical currents the terminal and ground are declared as boundary condition. And for heat transfer the surrounding air was set to 293K room temperature and the terminal and ground part was set to initial temperature 293K. Electrical characteristics along with side of temperature distribution because of applied current and voltage has been investigated thoroughly.

3.2 Simulation Result

From the simulation, micro fuse behavior in terms of temperature, potential, isothermal contour distribution due to the applied current through conductive electrode has been investigated. To examine the joule heating effect different current from 0.1A to 5.6A were applied at the terminal and the changes of temperature observed. **Figure 3.7** shows the surface temperature of micro fuse at current 5.6A and **Figure 3.8** shows the relation between applied current and temperature where temperature is increasing with the applied current and thus at 5.6A current the temperature of nearly 573K which is the melting point of Pb-Sn fuse material reached and the current conduction immediately interrupted due to the melting of fuse material. For applying current, current electrode has been used as ground and control electrode of the device has been used as a current terminal. From the figure at 5.6A current the maximum temperature of the triode micro fuse device occurred in the layer between electrode and fuse material and that melts the fuse material to interrupt the current.

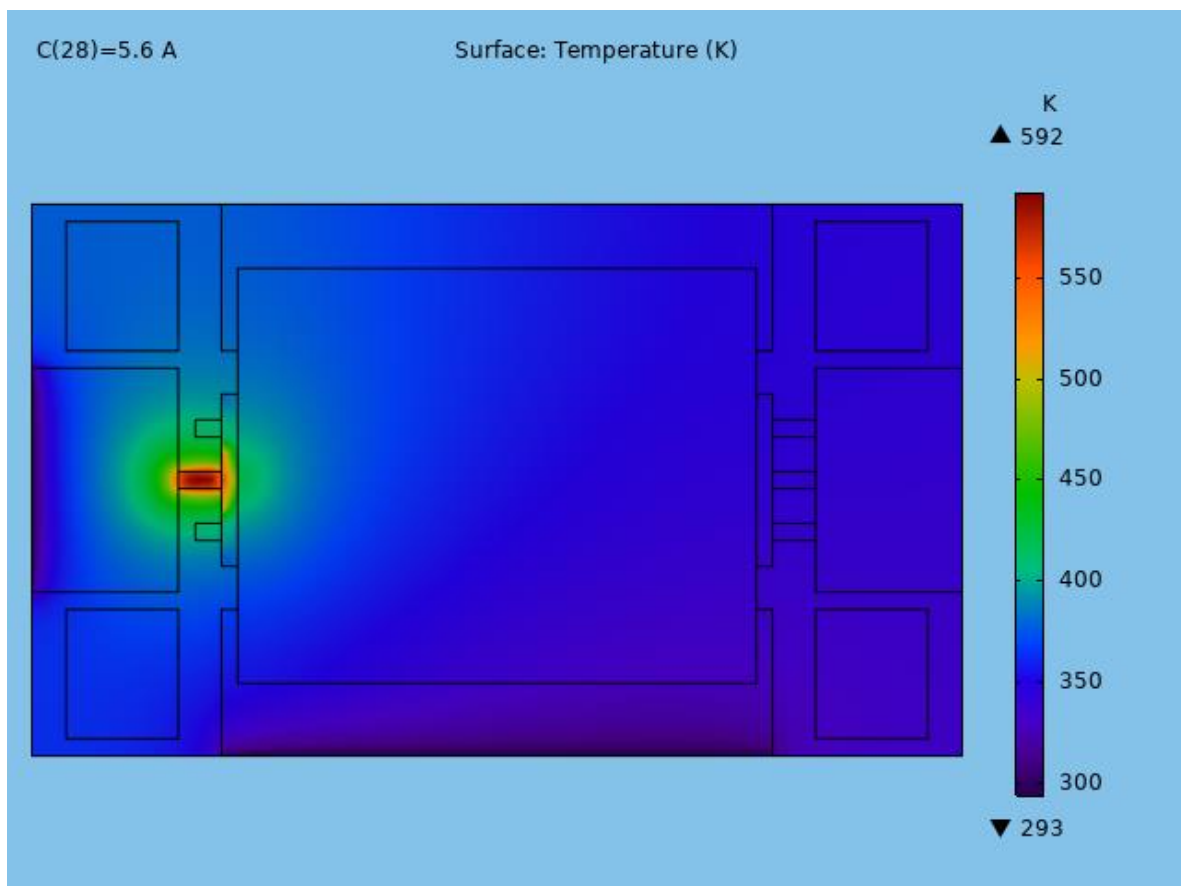


Figure 3.7. Temperature distribution of the triode micro fuse device maximum temperature and temperature profile

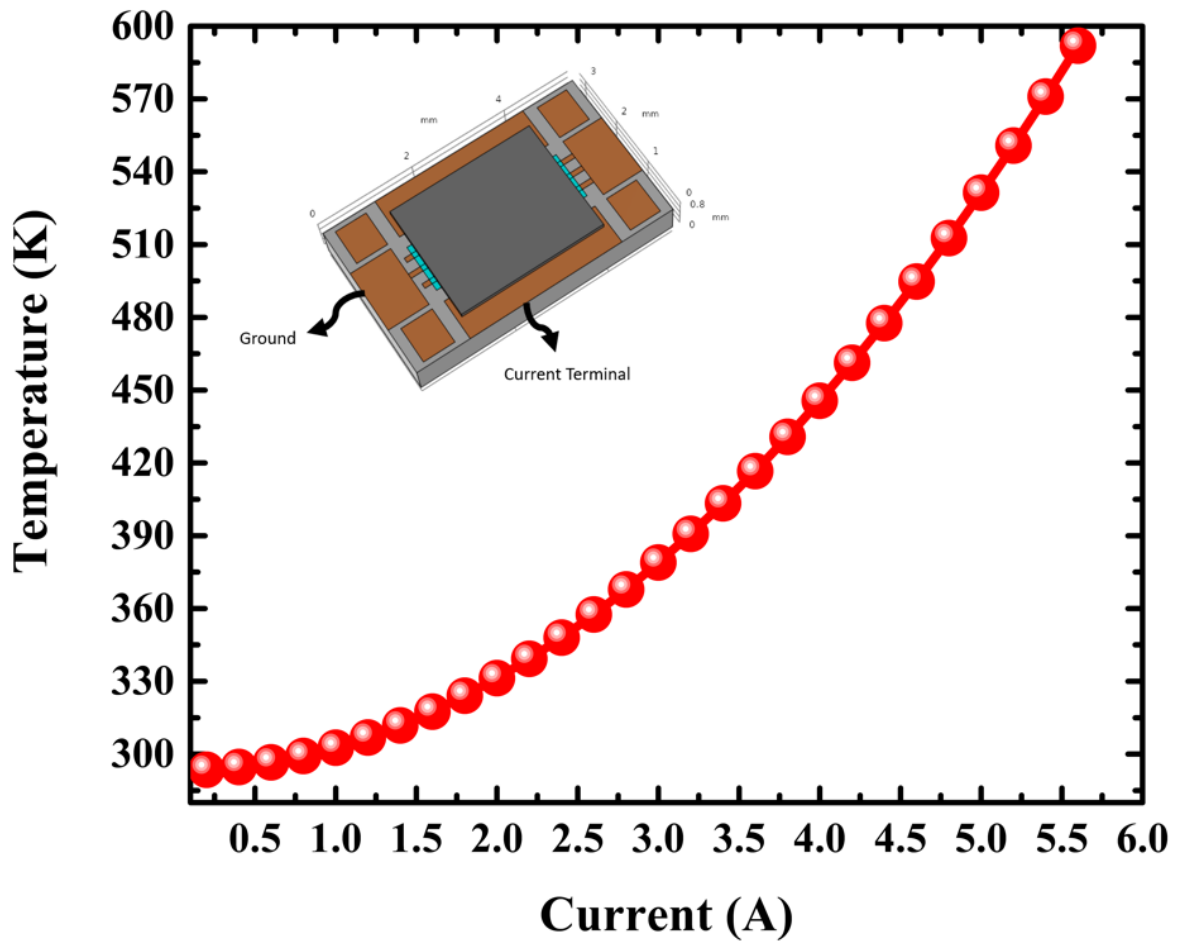


Figure 3.8. Temperature versus Current relationship of the micro fuse device by applying current through control and current electrode

Figure 3.9 shows the potential distribution of micro fuse device at current 5.6A and the isothermal contour distribution of the micro fuse at same current to understand the fuse mechanism at same configuration of the biasing point like **Figure 3.8**. From **Figure** it is evident that the voltage distribution is primarily identified in maximum temperature area stated at **Figure 3.8**. Also, from **Figure 3.10** the isothermal contour distribution verified the identical phenomena.

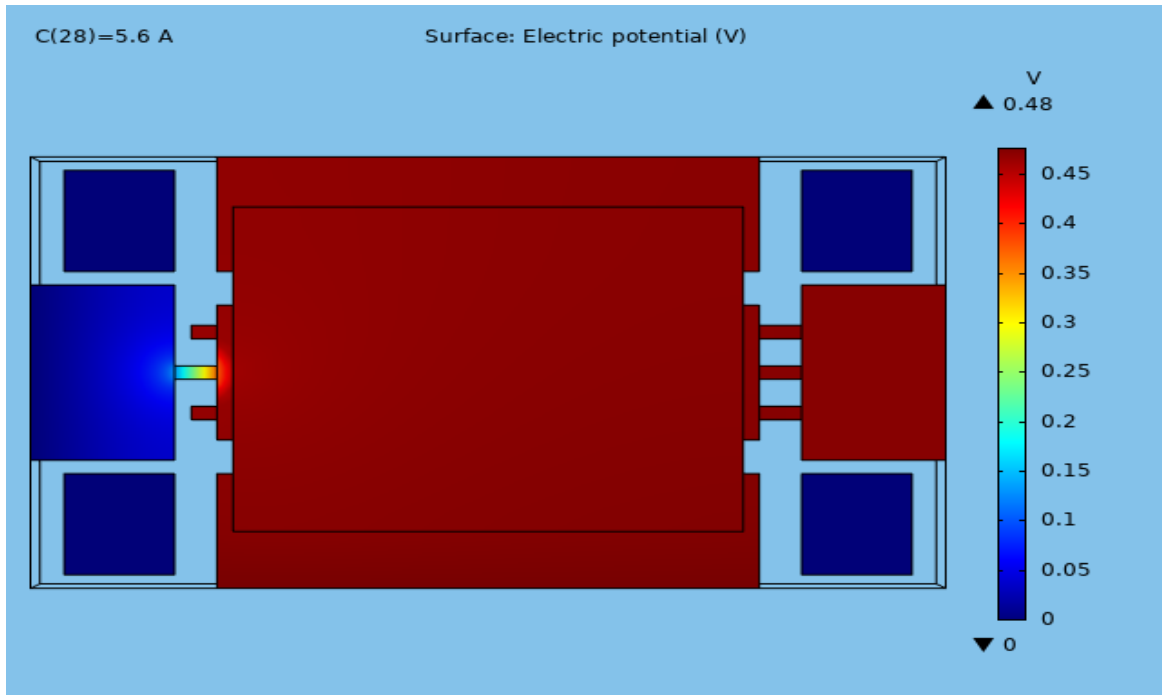


Figure 3.9. Voltage distribution of the triode micro fuse device between control and current electrode

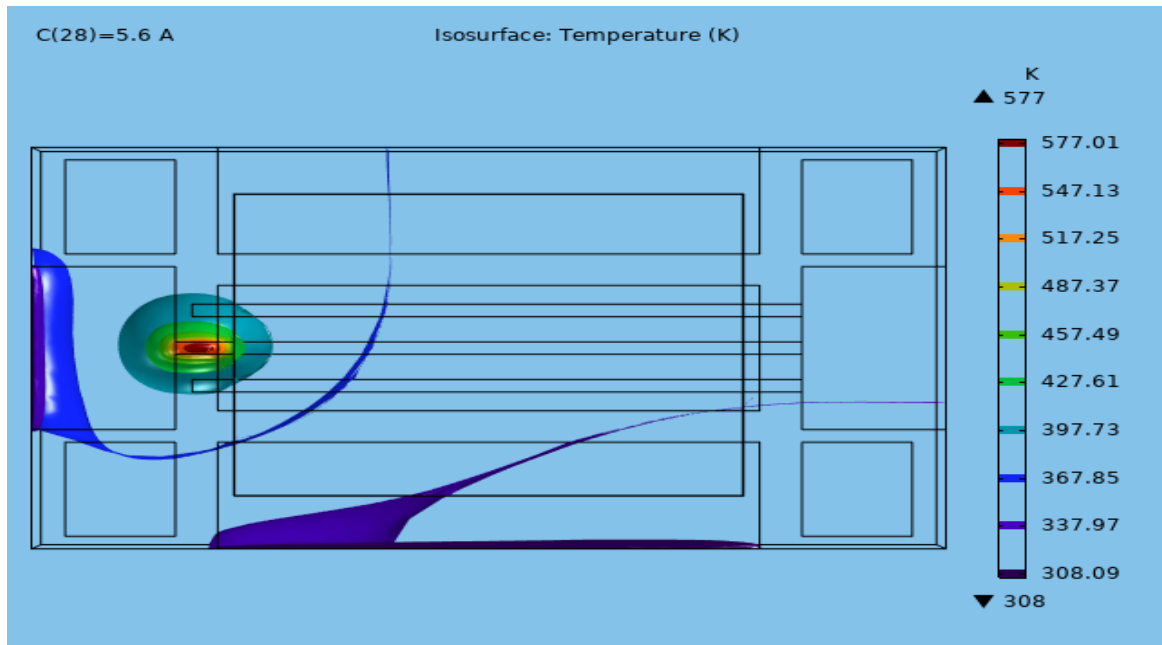


Figure 3.10. Isothermal contour distribution due to temperature on the micro fuse device

Fabrication of triode micro fuse

To develop the simulated triode micro fuse device on a highly rough alumina substrate, several experimental steps were carried out. For silver electrode deposition, Tungsten oxide heater deposition an ultra-high vacuum radio frequency magnetron sputtering technique has been used. For attaching the fuse material with these different techniques like thermocompression bonding, silver paste conductive coating techniques have been investigated. For good adhesion property, a thin film layer on the above of tungsten oxide film has been deposited also by using RF magnetron sputtering method. The whole process is reported in this chapter.

4.1 Substrate Preparation

The high roughness and hydrophobicity of commercially available alumina substrate is used to enhance the forming nanostructured film deposition. First, an extremely rough alumina substrate ($100 \times 100 \text{ mm}^2$) was washed for 5 minutes in ethanol, acetone, and isopropanol, then ultrasonicated for 15 minutes and dried with nitrogen gas, followed by heating the substrate in a hot plate at 100°C for 10 minutes. **Figure 4.1** shows the optical image of the alumina substrate.

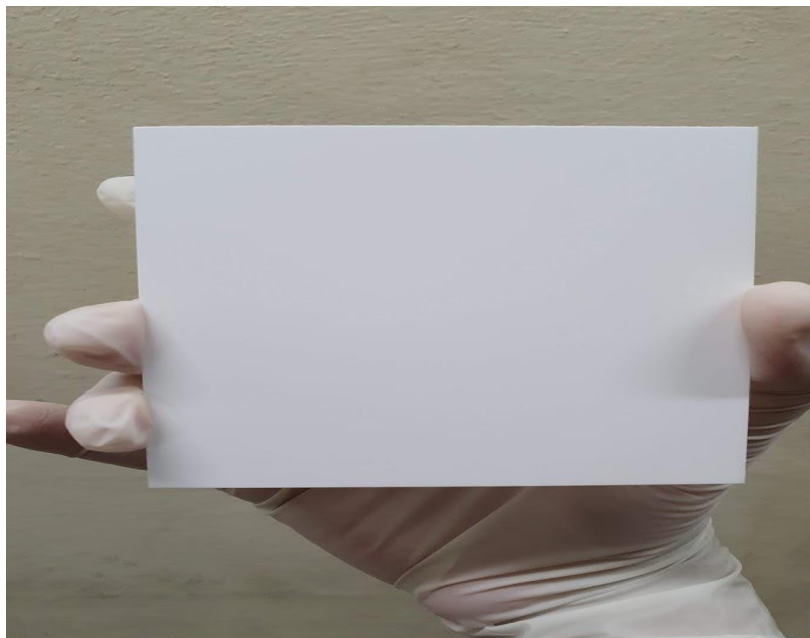


Figure 4.1. Optical image of Alumina Substrate

4.2 Silver Electrode Deposition

Silver electrode was sputtered on alumina substrate by RF magnetron sputtering and for this purpose Silver (99.9%) target (iTASCO, 2" Dia \times 1/8" Th) was used as a target material also shown in **Figure 4.2 (a)**. In the RF sputtering chamber, a gap of nearly 8cm was maintained between the substrate and the target. The distance between target and substrate has been shown in **Figure 4.2 (b)**.



Figure 4.2. (a) Optical image of Silver (Ag) Target (b) Distance between the substrate and target in the RF magnetron sputtering chamber

Silver was deposited at a deposition pressure of 8mTorr at a gas flow ratio of Ar:N₂ = 1:10 after the sputtering chamber was evacuated with a pressure of 10mTorr using a high vacuum rotary pump and followed by using a cryopump. The rate of deposition was nearly 1nm/Sec. The plasma was generated in the sputter chamber with a rf power of 130W and after the vacuum created, the temperature was recorded at 8K. **Table 4.1** summarizes the parameters used in the silver deposition. The rf magnetron sputtering process and the plasma formation has been shown in **Figure 4.3**. The optical image has been taken during the experimental procedures in the laboratory.

Table 4.1. Operating conditions of RF magnetron sputtering of Silver (Ag) target

Target	Ag (99.99%)
Target-Substrate distance	8cm
Base Pressure	10mTorr
RF Power	130W
Deposition Pressure	8mTorr
Temperature during deposition	8~10K
Deposition Rate	1 nm/Sec
Vacuum Condition	Cryopump and Rotary Pump combined

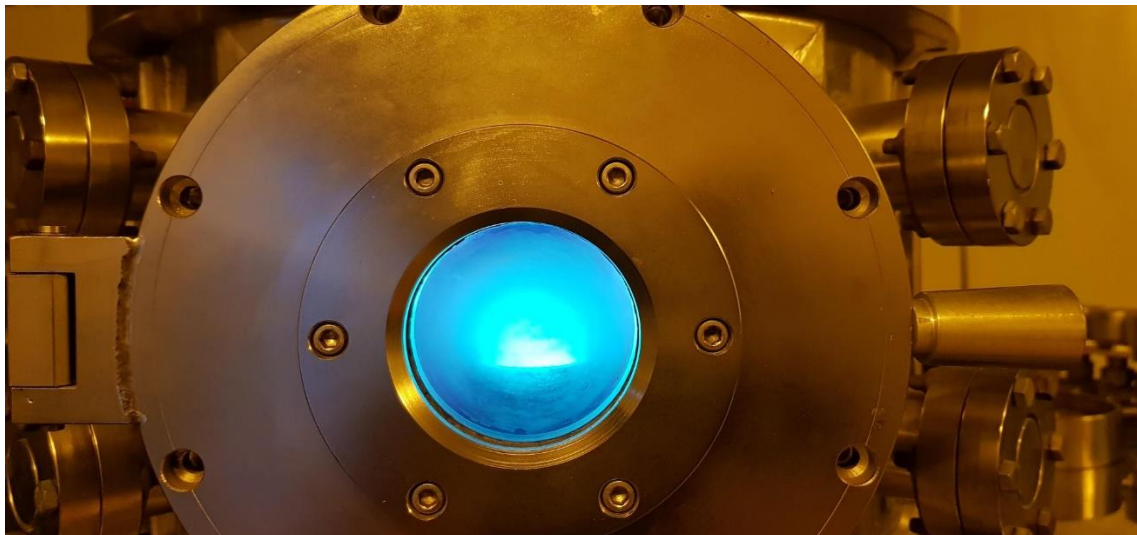


Figure 4.3. Optical image of RF magnetron sputtering plasma during deposition process

4.3 Heater Resistor deposition

For heater resistor deposition, Tungsten oxide (WO_3) was deposited on silver electrode. Tungsten oxide (99.9%) target (iTASCO, 2" Dia \times 1/8" Th) target was used in the sputtering process and operating conditions was varied to get the desired film thickness. The details of the parameters are shown in **Table 4.2**.

Table 4.2. Operating conditions of RF magnetron sputtering of Tungsten oxide (WO_3) target

Target	WO ₃ (99.99%)
Target-Substrate distance	6cm
Base Pressure	10mTorr
RF Power	100W
Deposition Pressure	8mTorr
Temperature during deposition	8~10K
Deposition Rate	0.15 nm/Sec
Vacuum Condition	Cryopump and Rotary Pump combined

4.4 Tin (Sn) deposition

To ensure the good adhesive characteristics between heater and fuse material (9:1 ratio based Pb-Sn fuse material), a thin film tin layer was necessary. In this purpose, Tin (99.9%) target (iTASCO, 2" Dia × 1/4" Th) was used for depositing very thin film of tin layer using RF sputtering. The details of the parameter used for tin deposition has been shown in Table 4.3.

Table 4.3. Operating conditions of RF magnetron sputtering of Tin (Sn) target

Target	Sn (99.99%)
Target-Substrate distance	8cm
Base Pressure	10mTorr
RF Power	25W
Deposition Pressure	8mTorr
Temperature during deposition	8~10K
Deposition Rate	0.8 nm/Sec
Vacuum Condition	Cryopump and Rotary Pump combined

The tungsten oxide and tin target has been shown in **Figure 4.4 (a)** and **(b)** respectively.

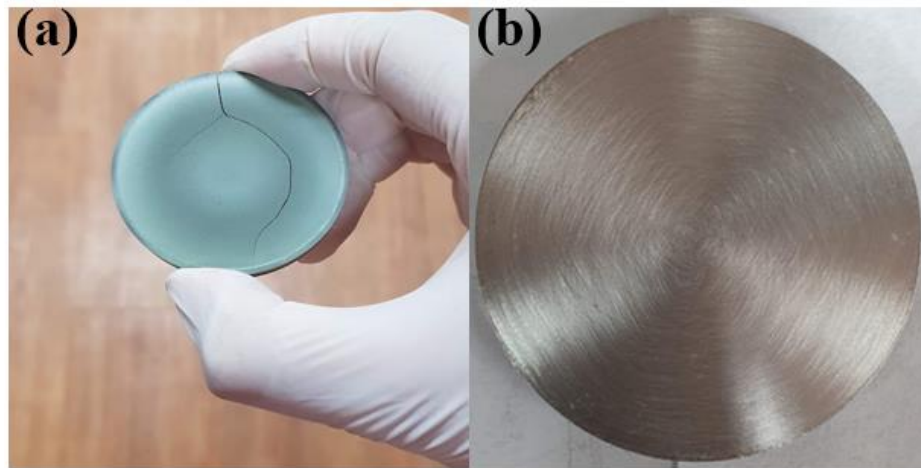


Figure 4.4. Optical image of (a) Tungsten oxide (WO_3) and (b) Tin (Sn) target for Sputtering

4.5 Surface Resistance Measurement

After depositing each film, it was necessary to measure the surface resistance of the deposited film. In this objective, KEITHLEY Four probe low resistance measurement system (SCS-4200) has been used and the optical image of the system has been shown in **Figure 4.5**.

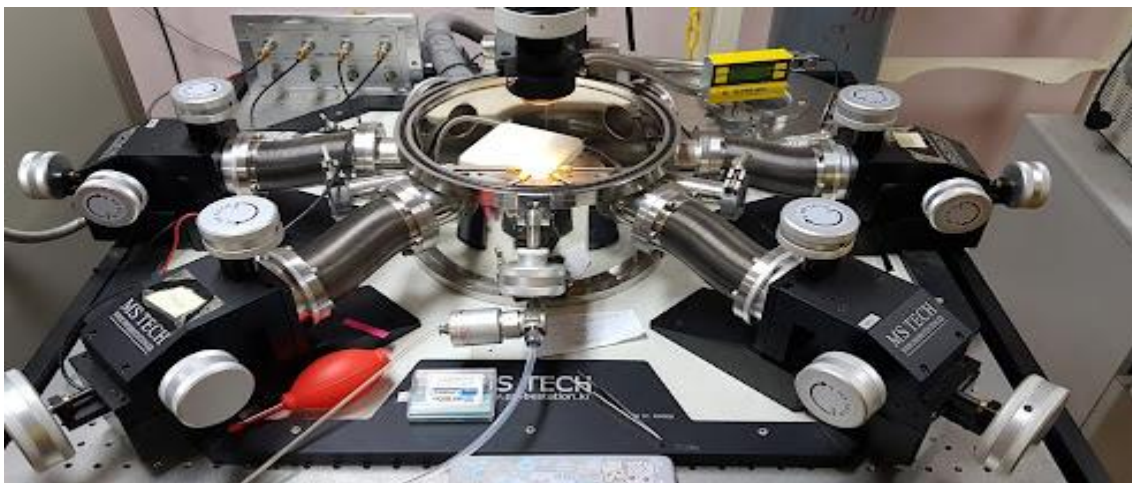


Figure 4.5. Four probe low resistance measurement system using KEITHLEY SCS-4200

4.6 The device fabrication process

For micro fuse testing and characterizing there requires a lot of devices to fabricate and electrical characteristics analysis becomes at ease. To meet this requirement, we developed and fabricated Ag metal electrode and WO_3 metal oxide heater on a rough alumina substrate with a RF magnetron sputtering in an ultra-high vacuum chamber. A highly rough electrically insulated alumina substrate ($100 \times 100 \text{ mm}^2$) with a thickness of 0.7mm, was cleaned for 5 minutes in acetone, isopropanol, and ethanol solution, cleaned with di-ionized (DI) water and then ultrasonicated (100°C) for 10 minutes. The width and length of the micro fuse is $5.4 \times 3.2 \text{ mm}^2$ and to fabricate we used shadow masking technology to deposit different metal and metal oxides nano film onto the alumina substrate as three different mask design have been showed in figure. Using mask conductive electrode of silver metal, heater material tungsten oxide and for bonding with fuse material a thin film of tin metal film sequentially deposited in a discrete thin film manner on the alumina substrate. The whole fabrication process is shown in **Figure 4.6**.

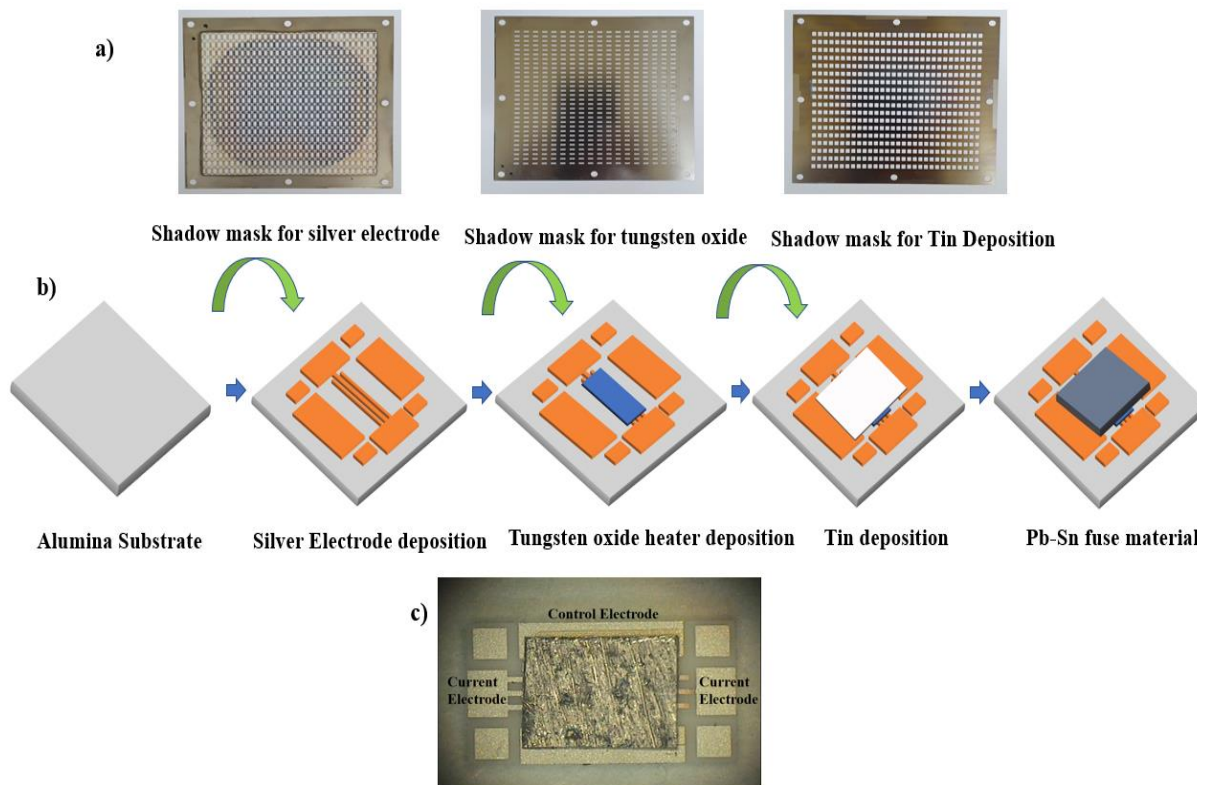


Figure 4.6. Schematic diagram of the sputtered triode micro fuse device nanofabrication steps a) different masking design to deposit different film of silver, tungsten oxide and tin film b) Fabrication process of sputtered thin film c) photography of micro fuse under Cam Scope

Electrical test and results

After fabricating the triode micro fuse device, its electrical characteristics has been investigated and analyzed. For measuring the electrical characteristics, a setup was also designed. The whole analyzation has been presented in this chapter.

5.1 Electrical characterization setup

A Test System like **Figure 5.1** was used to test the fusing performance of the triode micro fuse device. A regulated DC power supply (GP-4305TP, EZ Digital), a multimeter, and a polycarbonate testing chamber were used to construct the testing apparatus. Two silver paste electrodes were attached to the positive and negative electrodes of the testing system, respectively, prior to testing. The thin-film fuse mechanism tested in ambient settings by first applying a direct current between electrode 1 (current electrode) and electrode 3 (control electrode), then monitoring the voltage difference across the same terminal.

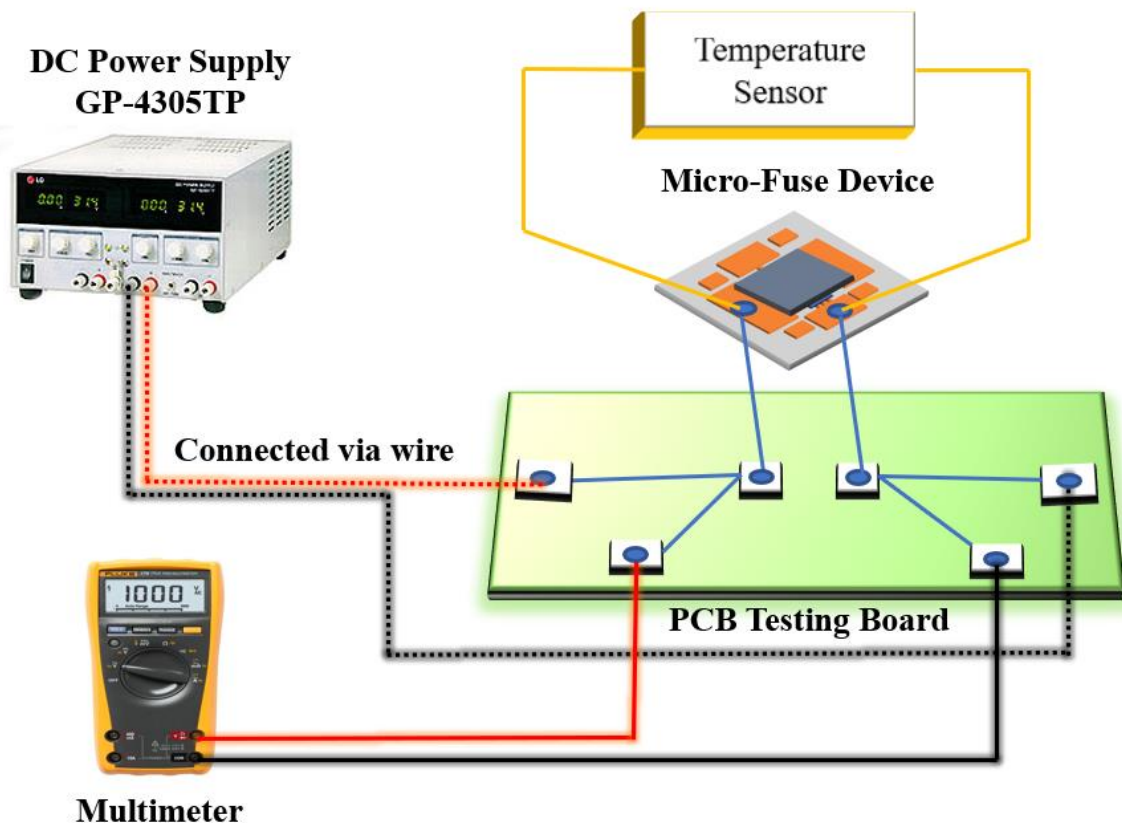


Figure 5.1. Testing setup of triode micro fuse device for electrical characterization

5.2 Electrical characterization Analysis

After depositing electrodes, heater resistor and tin film layer onto the substrate it was necessary to follow a sealing methods or bonding technique to attach the Pb-Sn alloy-based fuse material.

For making sample of the triode micro fuse device, two types of bonding technique have been followed and they are thermocompression bonding and epoxy bonding. Figure 5.2 shows the samples sealed with thermocompression bonding. The fuse alloy material melts at nearly 300°C temperature that is why the thermocompression bonding temperature is ranged between 220°C-275°C. In all cases the bond force was fixed to 88.3N.

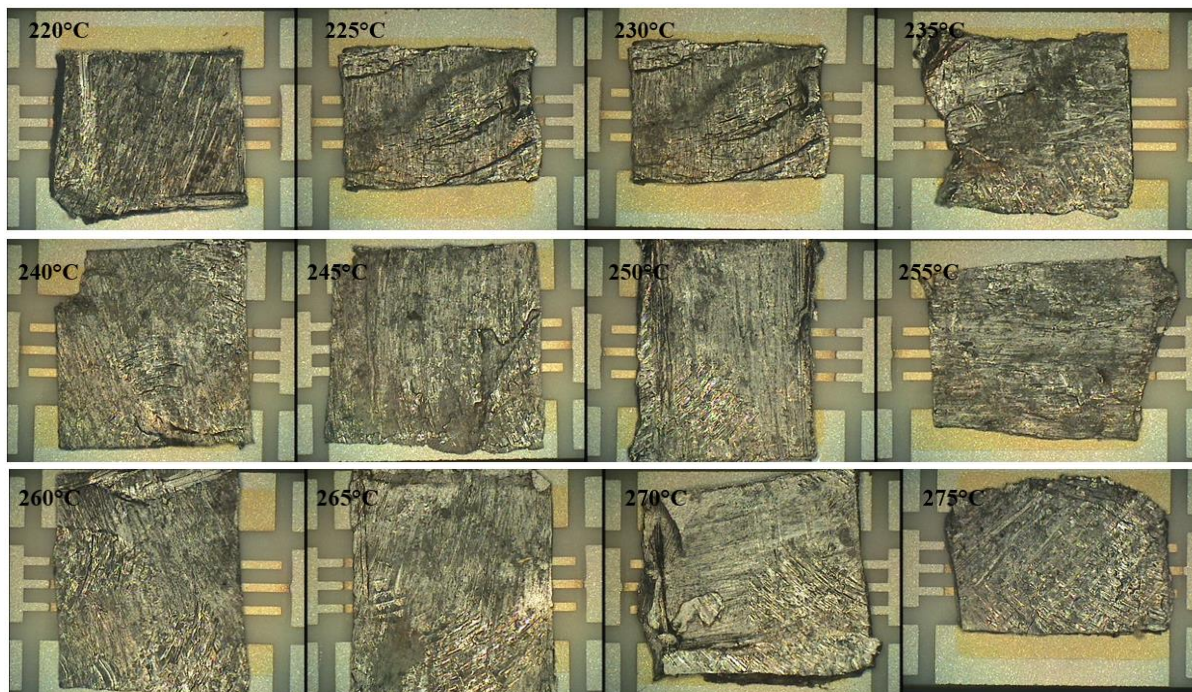


Figure 5.2. Using thermocompression bonding at different temperature to attach the fuse material with the substrate/electrode/heater layer to form triode micro fuse device

Metallic connections are produced between metal deposited substrates in thermocompression bonding by bringing them into proximity while simultaneously applying temperature and pressure. Regardless of surface roughness, the applied pressure must be high enough to bring the surfaces into atomic contact. Diffusion bonding is another name for the method [24].

For electric characterization, a current has been applied in the control electrode and current electrode and due to rapidly increasing current, the temperature also increased. That makes thermal shock phenomena, which arises from strain and that cracked the thermocompression bonding when temperature rises.

For bonding technique, epoxy bonding has been followed also and the bonded samples has been shown in **Figure 5.3**. In this technique, silver conducting paste has been used directly above the heater/tin layer and then the fuse alloy material placed onto that. After Epoxy bonding the device is set for testing.

The micro fuse device is electrically connected with the testing board via silver coating conductive paste.

When an applied current applied to the terminal and ground of the micro-fuse device at current electrode and control electrode, the current voltage relationship is recorded to manifest the fusing performance of the triode micro fuse device.

As can be seen from the **Figure 5.4**, the current applied in the device ranges from 0.1A to the near 5A current with an increment of 0.1A as per simulation assumption to reach the fuse material melting point. From the figure, the fuse element underwent three stages. In the first stage, the voltage almost linearly increases with applied current indicating an ohmic conductive characteristics.

The slightly increased resistance was ascribed to the temperature rise in the fuse element in a little amount.

The second stage occurred at about 2.5A current when the resistance increased at first and then decreased because of the mechanism of NTCR characteristics of Tungsten oxide material. That point towards the triode mechanism of tungsten oxide NTC metal oxide working above the conducting electrode and thus protecting the device from high joule heating caused by applied current.

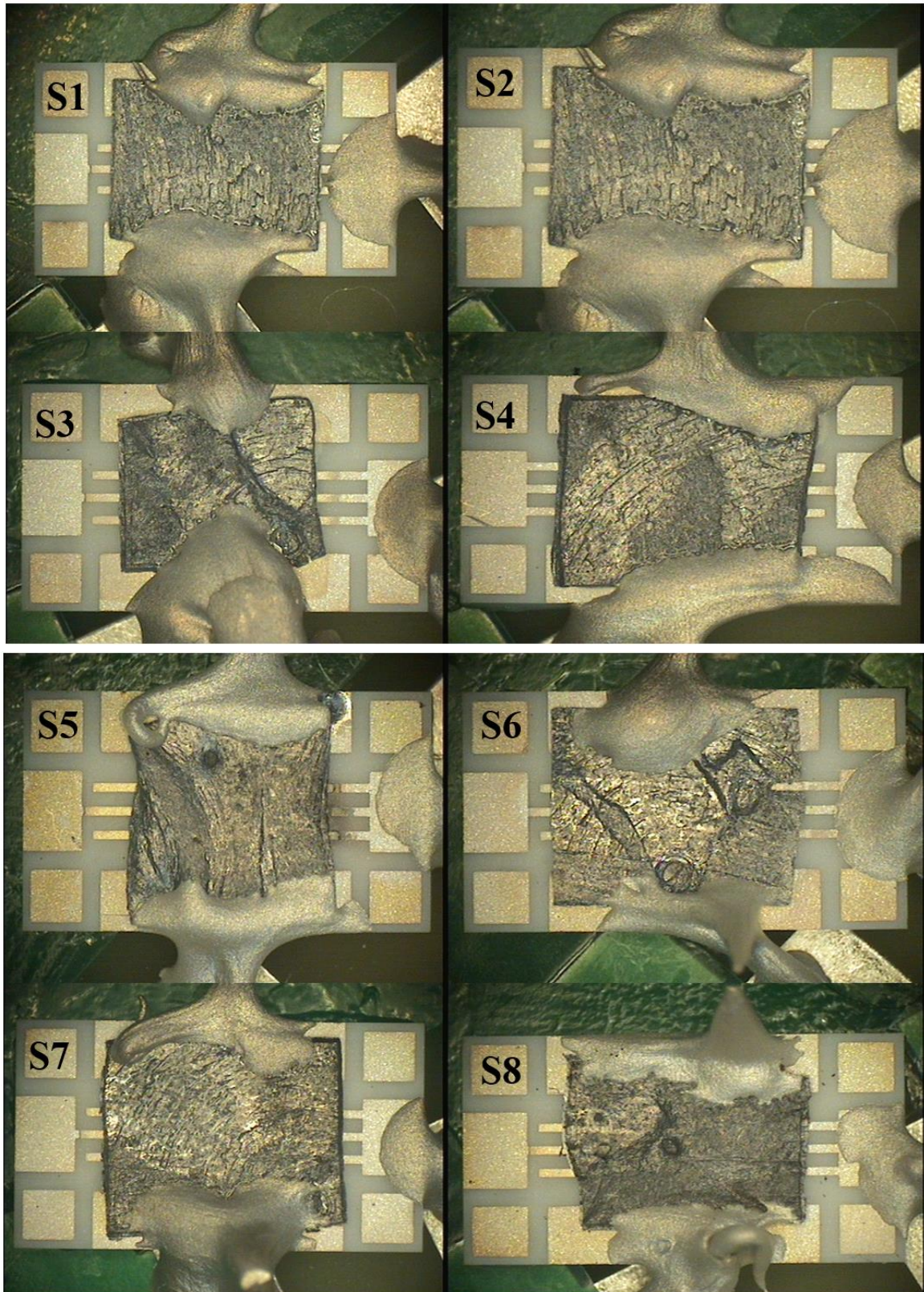


Figure 5.3. Using silver conductive coating paste to form the bonding of fuse material with substrate/electrode/heater layer to form triode micro fuse device

The third stage is about approaching towards the limiting current, and the resistance increases sharply and in consequence the temperature also increases with the applied current and the voltage increases sharply with increasing the current and the temperature at about 593K reached and the circuit disconnected thus current is interrupted by melting the fuse material. The current turns immediately to 0A through the circuit.

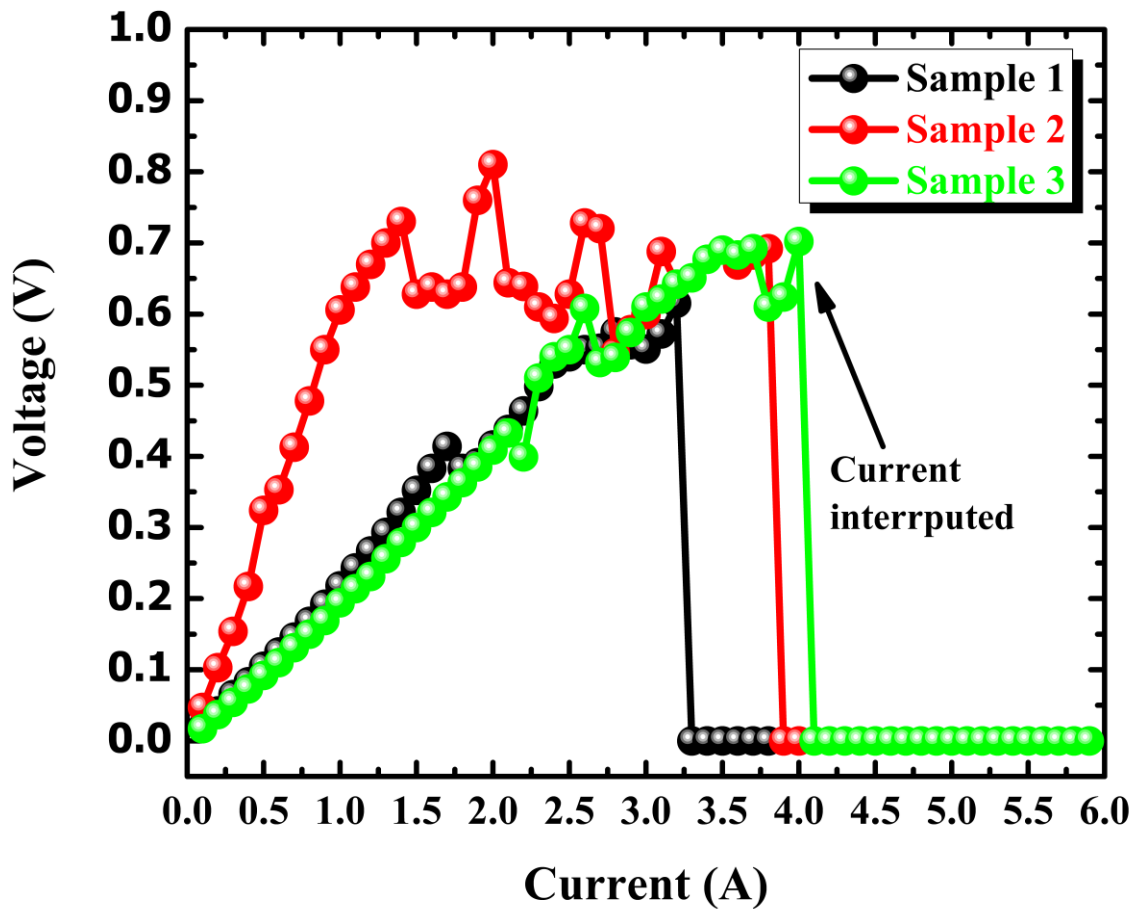


Figure 5.4. Current-Voltage (I-V) characteristics of triode micro fuse device

Figure 5.5 shows the relationship between current and temperature of the triode micro fuse device. With applied current the temperature increases and follows the simulated data almost in a same manner. The figure also shows the extrapolated data after 4A current, which is because the sampled device can not endure more current flow through the device due to thermal shocking and cracking behavior of the connectivity electrode of the sample and testing chamber.

From the figure it is evident that, the simulated temperature profile is aligned with the experimental data.

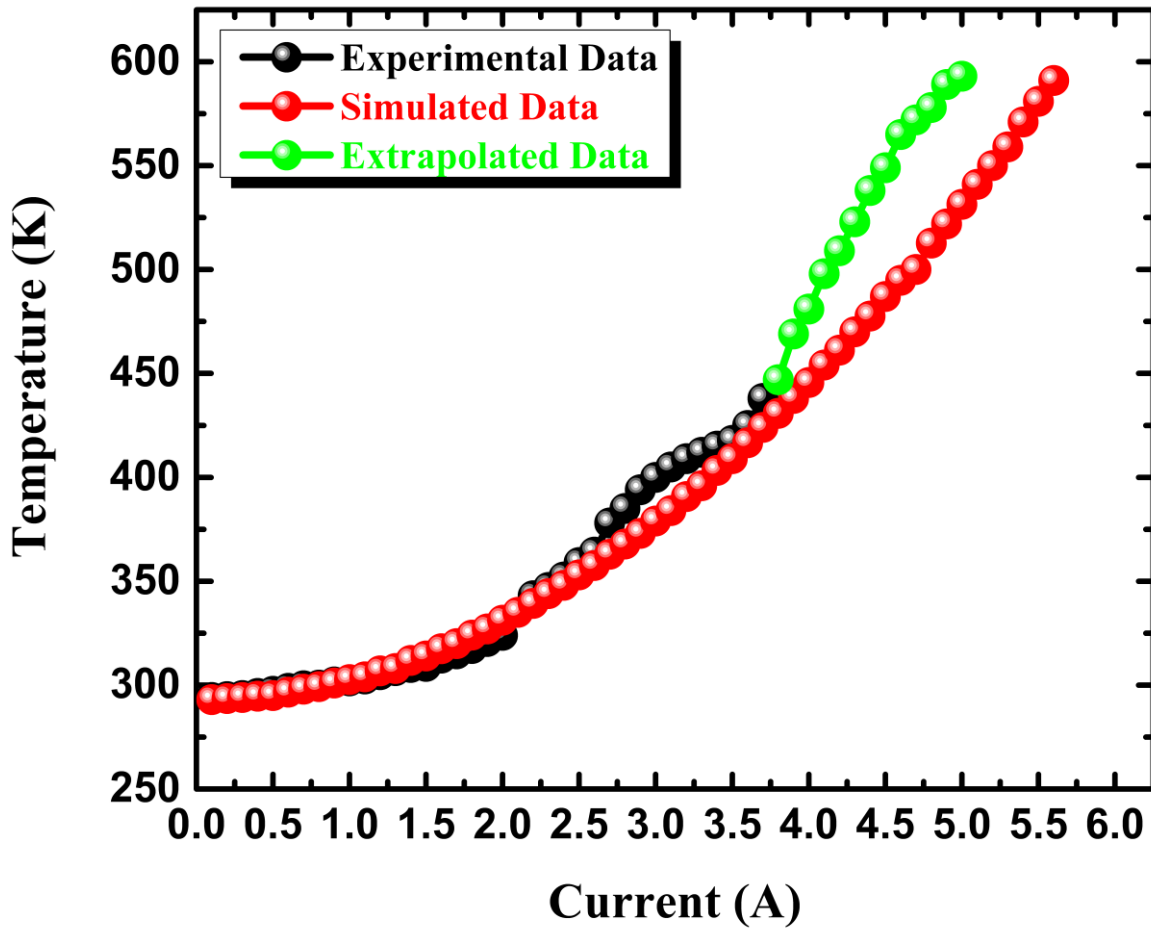


Figure 5.5. Current-temperature characteristics of triode micro fuse

This novel triode micro fuse is designed to protecting the high current portable secondary battery and **Figure 5.6** reveals the blown mechanism of this device at current rating 5A. **Figure 5.6 (a)** shows the micro fuse before current has been applied. When current has been applied the point where maximum temperature estimated (as per the simulation) blew, as shown in **Figure 5.6 (b)**.



Figure 5.6. Triode micro fuse device blown at 5A applied current (a) before applied current (b) after applying the blown fuse

Conclusions and future work

6.1 Conclusions

In this current study, we fabricated a novel triode micro fuse device that can be used as a protective device for portable secondary battery like li-ion battery from overcharging which causes overvoltage and overcurrent. Metal oxides which show the negative temperature coefficient of resistance characteristics are normally used as heater resistance and in this study, we have used a NTC characteristics-based metal oxide, which is tungsten oxide as a heater in our proposed micro fuse structure which enables the advantages of safely flowing high current in a smaller fuse area compared to micro fuse current rating in other words can control more electrical power. The transient behavior of NTC material has been modelled using PSPICE ABM which making it possible to simulate the transient behavior of temperature due to joule heating effect of the heater material and the theoretical background suggests an analytical model to visualize the current conduction, heat transfer physics of the micro fuse device. The analytical model has been validated by MEMS based COMSOL Multiphysics which provides the geometry of the device with Joule heating Multiphysics platform. We proposed a complete device structure using the analytical model that combines the electric current and heat transfer module for the triode micro fuse device. We have analyzed the electric current and voltage profile with temperature profile for the estimation of our result and by motivating from the model we have fabricate the micro fuse device experimentally. The simulated data shows that at nearly 5A current the micro fuse device reaches at nearly 593K temperature (300°C) which breaks the circuit quickly and forced the current to stop flowing through the circuit. As nanofabrication technique we have used RF magnetron sputtering for depositing different layer and we have used two bonding techniques to bond the device with the fuse material. The electrical characterization of the micro fuse device shows that, it follows almost same characteristics with the simulated data and the current voltage curve shows the same phenomena. Due to thermal shocking and strain between the fuse material and the conducting path, the device faces some early breakdown in the circuit, but an interpolated data shows that at nearly 5A current the circuit got disconnected by blowing the fuse immediately. From the analysis it is clearly evident that, our fabricated device could be a perfect candidate for using as a protecting device and control high current applications by protecting them.

6.2 Future work and suggestions

We are undergoing this work for more power and current control mechanism. We have already modelled and fabricated the triode micro fuse device for 5A current control capability. This time, we are targeting more high power and current control by optimizing some physical parameter.

In this regard, the following issues we can deal as our future works-

- Since in this study, we have faced thermal shocking behavior with cracking behavior, we will work to mitigate this problem in our new structure
- We have already used epoxy bonding to form bond between fuse material and device, but we will use screen printing silver technique in our next work for durability and adhesiveness.
- The current electrode shape could be a vital role for enabling the capability of controlling more current in the micro fuse device. In this case, using COMSOL geometry the shape of the current electrode will be optimized also.

6.3 List of Publications by the Author

Journal Submission

1. Shovon Talukder, Hyeon Cheol Kim, “**Computational Analysis of a Novel Triode Micro Fuse with a WO₃ Heater**” “**Mathematical Problems in Engineering**” (1.305), under review

Conference Publication

1. Shovon Talukder, Hyeon Cheol Kim, “**A computational study of a three-electrode based micro fuse structure**” “IEIE” “ISSN 2005-0496”
2. Shovon Talukder, Hyeon Cheol Kim, “**A Novel Triode Micro Fuse Structure with WO₃ Heater**” “6th International Conference on Advanced Electro materials” “ICAE 2021”

References

- [1] X. Feng, M. Ouyang, X. Liu, L. Lu, Y. Xia, X. He, Thermal runaway mechanism of lithium ion battery for electric vehicles: A review, *Energy Storage Mater.* 10 (2018) 246–267. <https://doi.org/10.1016/j.ensm.2017.05.013>.
- [2] Y. Chen, Y. Kang, Y. Zhao, L. Wang, J. Liu, Y. Li, Z. Liang, X. He, X. Li, N. Tavajohi, B. Li, A review of lithium-ion battery safety concerns: The issues, strategies, and testing standards, *J. Energy Chem.* 59 (2021) 83–99. <https://doi.org/10.1016/j.jechem.2020.10.017>.
- [3] X.M. Feng, X.P. Ai, H.X. Yang, A positive-temperature-coefficient electrode with thermal cut-off mechanism for use in rechargeable lithium batteries, *Electrochem. Commun.* 6 (2004) 1021–1024. <https://doi.org/10.1016/j.elecom.2004.07.021>.
- [4] A. Wright and P.G. Newbery, *Electric Fuses*, (1386) 283.
- [5] J.G. Leach, P.G. Newbery, A. Wright, Analysis of High-Rupturing-Capacity Fuselink Prearcing Phenomana By a Finite-Difference Method., *Proc. Inst. Electr. Eng.* 120 (1973) 987–993. <https://doi.org/10.1049/piee.1973.0220>.
- [6] B.P. Singh, B.K. Jena, S. Bhattacharjee, L. Besra, Development of oxidation and corrosion resistance hydrophobic graphene oxide-polymer composite coating on copper, *Surf. Coatings Technol.* 232 (2013) 475–481. <https://doi.org/10.1016/j.surfcoat.2013.06.004>.
- [7] Z. Jia, (12) United States Patent, 2 (2017).
- [8] A.Ü. Keskin, A simple analog behavioural model for NTC thermistors including selfheating effect, *Sensors Actuators, A Phys.* 118 (2005) 244–247. <https://doi.org/10.1016/j.sna.2004.06.034>.
- [9] S.E. DORRIS, T.O. MASON, Electrical Properties and Cation Valencies in Mn₃O₄, *J. Am. Ceram. Soc.* 71 (1988) 379–385. <https://doi.org/10.1111/j.1151-2916.1988.tb05057.x>.
- [10] S.E. Lee, Y. Sohn, K. Cho, D. Kim, S.H. Park, M. Bae, D. Kim, Y. Kim, I.T. Han, H.J. Kim, Suppression of negative temperature coefficient of resistance of multiwalled nanotube/silicone rubber composite through segregated conductive network and its application to laser-printing fusing element, *Org. Electron.* 37 (2016) 371–378. <https://doi.org/10.1016/j.orgel.2016.07.010>.
- [11] H. Altenburg, O. Mrooz, J. Plewa, O. Shpotyuk, M. Vakiv, Semiconductor ceramics for NTC thermistors: The reliability aspects, *J. Eur. Ceram. Soc.* 21 (2001) 1787–1791. [https://doi.org/10.1016/S0955-2219\(01\)00116-9](https://doi.org/10.1016/S0955-2219(01)00116-9).
- [12] H. Zheng, J.Z. Ou, M.S. Strano, R.B. Kaner, A. Mitchell, K. Kalantar-Zadeh, Nanostructured tungsten oxide - Properties, synthesis, and applications, *Adv. Funct. Mater.* 21 (2011) 2175–2196. <https://doi.org/10.1002/adfm.201002477>.
- [13] H.S. Shim, J.W. Kim, Y.E. Sung, W.B. Kim, Electrochromic properties of tungsten oxide nanowires fabricated by electrospinning method, *Sol. Energy Mater. Sol. Cells.*

- 93 (2009) 2062–2068. <https://doi.org/10.1016/j.solmat.2009.02.008>.
- [14] G. Leftheriotis, S. Papaefthimiou, P. Yianoulis, The effect of water on the electrochromic properties of WO₃ films prepared by vacuum and chemical methods, *Sol. Energy Mater. Sol. Cells*. 83 (2004) 115–124. <https://doi.org/10.1016/j.solmat.2004.02.019>.
- [15] W.L. Kwong, N. Savvides, C.C. Sorrell, Electrodeposited nanostructured WO₃ thin films for photoelectrochemical applications, *Electrochim. Acta*. 75 (2012) 371–380. <https://doi.org/10.1016/j.electacta.2012.05.019>.
- [16] K.S. Ahn, S.H. Lee, A.C. Dillon, C.E. Tracy, R. Pitts, The effect of thermal annealing on photoelectrochemical responses of WO₃ thin films, *J. Appl. Phys.* 101 (2007) 1–4. <https://doi.org/10.1063/1.2729472>.
- [17] K. Hari Krishna, O.M. Hussain, C.M. Julien, Electrochromic properties of nanocrystalline WO₃ thin films grown on flexible substrates by plasma-assisted evaporation technique, *Appl. Phys. A Mater. Sci. Process.* 99 (2010) 921–929. <https://doi.org/10.1007/s00339-010-5681-5>.
- [18] H. Zheng, A.Z. Sadek, K. Latham, K. Kalantar-Zadeh, Nanoporous WO₃ from anodized RF sputtered tungsten thin films, *Electrochem. Commun.* 11 (2009) 768–771. <https://doi.org/10.1016/j.elecom.2009.01.033>.
- [19] X. Song, G. Yang, F. Nie, A micro fuse realized by integrating Al/CuO-based nanoenergetic materials on a micro wire, *Mater. Sci. Forum*. 694 (2011) 249–255. <https://doi.org/10.4028/www.scientific.net/MSF.694.249>.
- [20] Y.T. Chen, S.W. Kang, C.C. Hsu, J.W. Lin, Micro fuse fabrication and testing, *Tamkang J. Sci. Eng.* 10 (2007) 173–176. <https://doi.org/10.6180/jase.2007.10.2.15>.
- [21] M. Dohi, T. Tsujioka, Thin-film micro-fuse with a novel structure prepared by Ag vapor deposition modulation based on organic photochromism, *Appl. Phys. Express*. 6 (2013). <https://doi.org/10.7567/APEX.6.091601>.
- [22] S. Jagtap, S. Rane, S. Gosavi, D. Amalnerkar, Study on I-V characteristics of lead free NTC thick film thermistor for self heating application, *Microelectron. Eng.* 88 (2011) 82–86. <https://doi.org/10.1016/j.mee.2010.08.025>.
- [23] B. Beads, G.C. Beads, R. Beads, M.G. Probes, G. Probes, G. Rods, B. Enclosures, S. Mounts, Ntc thermistors, 1 (1823).
- [24] N. Malik, K. Schjølberg-Henriksen, E. Poppe, M.M.V. Taklo, T.G. Finstad, Al-Al thermocompression bonding for wafer-level MEMS sealing, *Sensors Actuators, A Phys.* 211 (2014) 115–120. <https://doi.org/10.1016/j.sna.2014.02.030>.